

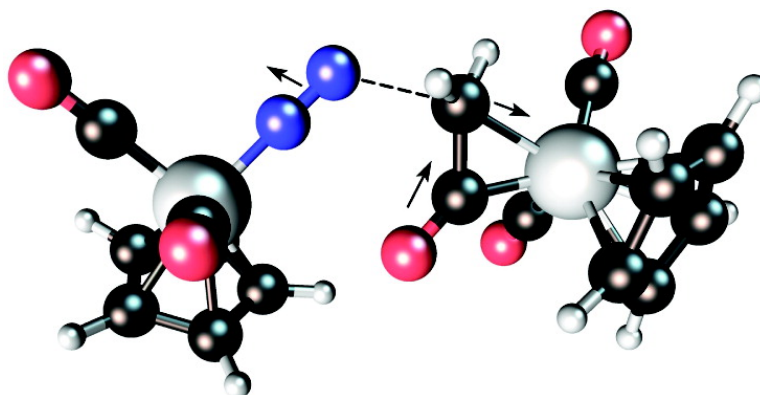
Article

Spectroscopic Detection and Theoretical Confirmation of the Role of $\text{Cr}(\text{CO})(\text{CR})$ and $\cdot\text{Cr}(\text{CO})(\text{ketene})(\text{CR})$ as Intermediates in Carbonylation of NNCHSiMe to OCCHSiMe by $\cdot\text{Cr}(\text{CO})(\text{CR})$ ($\text{R} = \text{H}, \text{CH}$)

George C. Fortman, Tams Kgl, Qian-Shu Li, Xiuhui Zhang, Henry F. Schaefer, Yaoming Xie, R. Bruce King, Joshua Telser, and Carl D. Hoff

J. Am. Chem. Soc., **2007**, 129 (46), 14388-14400 • DOI: 10.1021/ja075008o • Publication Date (Web): 26 October 2007

Downloaded from <http://pubs.acs.org> on February 13, 2009



More About This Article

Additional resources and features associated with this article are available within the HTML version:

- Supporting Information
- Links to the 4 articles that cite this article, as of the time of this article download
- Access to high resolution figures
- Links to articles and content related to this article
- Copyright permission to reproduce figures and/or text from this article

[View the Full Text HTML](#)



ACS Publications
 High quality. High impact.

Spectroscopic Detection and Theoretical Confirmation of the Role of $\text{Cr}_2(\text{CO})_5(\text{C}_5\text{R}_5)_2$ and $\cdot\text{Cr}(\text{CO})_2(\text{ketene})(\text{C}_5\text{R}_5)$ as Intermediates in Carbonylation of $\text{N}=\text{N}=\text{CHSiMe}_3$ to $\text{O}=\text{C}=\text{CHSiMe}_3$ by $\cdot\text{Cr}(\text{CO})_3(\text{C}_5\text{R}_5)$ ($\text{R} = \text{H}, \text{CH}_3$)

George C. Fortman,[†] Tamás Kégl,^{*,‡} Qian-Shu Li,^{*,§} Xiuhui Zhang,[§] Henry F. Schaefer III,^{||} Yaoming Xie,^{||} R. Bruce King,^{*,||} Joshua Telser,^{*,⊥} and Carl D. Hoff^{*,†}

Contribution from the Department of Chemistry, University of Miami, Coral Gables, Florida, 33126, Department of Organic Chemistry, University of Pannonia, Veszprém, Hungary, The Institute for Chemical Physics, Beijing Institute of Technology, Beijing, 100081 People's Republic of China, Department of Chemistry and Center for Computational Chemistry, University of Georgia, Athens, Georgia 30606, and Department of Biological, Chemical and Physical Sciences, Roosevelt University, Chicago, Illinois 60605

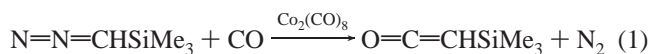
Received July 6, 2007; E-mail: c.hoff@miami.edu

Abstract: Conversion of $\text{N}=\text{N}=\text{CHSiMe}_3$ to $\text{O}=\text{C}=\text{CHSiMe}_3$ by the radical complexes $\cdot\text{Cr}(\text{CO})_3\text{C}_5\text{R}_5$ ($\text{R} = \text{H}, \text{CH}_3$) derived from dissociation of $[\text{Cr}(\text{CO})_3(\text{C}_5\text{R}_5)]_2$ have been investigated under CO, Ar, and N_2 atmospheres. Under an Ar or N_2 atmosphere the reaction is stoichiometric and produces the $\text{Cr}=\text{Cr}$ triply bonded complex $[\text{Cr}(\text{CO})_2(\text{C}_5\text{R}_5)]_2$. Under a CO atmosphere regeneration of $[\text{Cr}(\text{CO})_3(\text{C}_5\text{R}_5)]_2$ ($\text{R} = \text{H}, \text{CH}_3$) occurs competitively and conversion of diazo to ketene occurs catalytically as well as stoichiometrically. Two key intermediates in the reaction, $\cdot\text{Cr}(\text{CO})_2(\text{ketene})(\text{C}_5\text{R}_5)$ and $\text{Cr}_2(\text{CO})_5(\text{C}_5\text{R}_5)_2$ have been detected spectroscopically. The complex $\cdot\text{Cr}(\text{CO})_2(\text{O}=\text{C}=\text{CHSiMe}_3)(\text{C}_5\text{Me}_5)$ has been studied by electron spin resonance spectroscopy in toluene solution: $g(\text{iso}) = 2.007$; $A(^{53}\text{Cr}) = 125$ MHz; $A(^{13}\text{CO}) = 22.5$ MHz; $A(\text{O}=\text{C}=\text{CHSiMe}_3) = 12.0$ MHz. The complex $\text{Cr}_2(\text{CO})_5(\text{C}_5\text{H}_5)_2$, generated in situ, does not show a signal in its ^1H NMR and reacts relatively slowly with CO. It is proposed to be a ground-state triplet in keeping with predictions based on high level density functional theory (DFT) studies. Computed vibrational frequencies are also in good agreement with experimental data. The rates of CO loss from $^3\text{Cr}_2(\text{CO})_5(\text{C}_5\text{H}_5)_2$ producing $^1[\text{Cr}(\text{CO})_2(\text{C}_5\text{H}_5)]_2$ and CO addition to $^3\text{Cr}_2(\text{CO})_5(\text{C}_5\text{H}_5)_2$ producing $^1[\text{Cr}(\text{CO})_3(\text{C}_5\text{H}_5)]_2$ have been measured by kinetics and show $\Delta H^\ddagger \cong 23$ kcal mol⁻¹ for both processes. Enthalpies of reduction by Na/Hg under CO atmosphere of $[\text{Cr}(\text{CO})_n(\text{C}_5\text{H}_5)]_2$ ($n = 2, 3$) have been measured by solution calorimetry and provide data for estimation of the $\text{Cr}=\text{Cr}$ bond strength in $[\text{Cr}(\text{CO})_2(\text{C}_5\text{H}_5)]_2$ as 72 kcal mol⁻¹. The complex $[\text{Cr}(\text{CO})_2(\text{C}_5\text{H}_5)]_2$ does not readily undergo ^{13}CO exchange at room temperature or 50 °C implying that $^3\text{Cr}_2(\text{CO})_5(\text{C}_5\text{H}_5)_2$ is not readily accessed from the thermodynamically stable complex $[\text{Cr}(\text{CO})_2(\text{C}_5\text{H}_5)]_2$. A detailed mechanism for metalloradical based conversion of diazo and CO to ketene and N_2 is proposed on the basis of a combination of experimental and theoretical data.

1. Introduction

The generation of ketenes ($\text{R}_2\text{C}=\text{C}=\text{O}$) is important because of their prominent role in organic synthesis.¹ In this connection diazoalkanes ($\text{R}_2\text{C}=\text{N}=\text{N}$) can serve as ketene sources by their thermal or photochemical reaction with CO. Ungváry and co-workers² have recently shown that carbonylation of (tri-

methylsilyl)diazomethane is catalyzed by $\text{Co}_2(\text{CO})_8$ and selectively produces (trimethylsilyl)ketene:



Such methods provide an attractive route to the in situ generation of ketenes. However the mechanism of the metal-catalyzed conversion of diazoalkanes to ketenes is not fully understood even though the coordination chemistry of both diazoalkanes and ketenes has been extensively investigated.³

A number of fascinating aspects of ketene coordination chemistry have been discovered. Grotjahn and co-workers⁴ have demonstrated coordination of ketenes by both C,C- and C,O-

(3) Zollinger, H. *Diazo Chemistry*; VCH: Weinheim, Germany, 1995.

[†] University of Miami.

[‡] University of Pannonia.

[§] Beijing Institute of Technology.

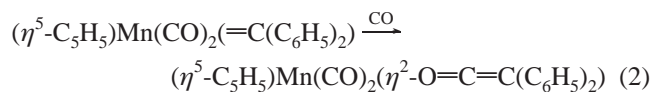
^{||} University of Georgia.

[⊥] Roosevelt University.

(1) Tidwell, T. T. *Ketenes*. Wiley, New York, 1995.

(2) (a) Ungvári, N.; Kégl, T.; Ungváry, F. *J. Mol. Catal. A: Chem.* **2004**, *219*, 7. (b) Kégl, T.; Ungváry, F. *J. Organomet. Chem.* **2007**, *692*, 1825. (c) Tuba, R.; Ungváry, F. *J. Mol. Catal. A: Chem.* **2003**, *203*, 59. (d) Fördös, E.; Ungvári, N.; Kégl, T.; Ungváry, F. *J. Eur. J. Inorg. Chem.* **2006**, 1875.

bonding modes to *trans*-ClIr[P(ⁱPr)₃]₂. However, related Ir(I) complexes containing chelating phosphines were also shown to split bound ketene ligands to CO and carbene units in reversible reactions.⁵ Hermann and co-workers⁶ reported the synthesis and structures of η^2 -ketene complexes by slow high-pressure carbonylation of metallocarbenes as shown in eq 2:



The stability of the η^2 -ketene bonding mode was indicated by the ability of such metal complexes to withstand high pressures of CO without undergoing ligand displacement. Related η^2 -ketene complexes have also been prepared by the reaction of photogenerated $(\eta^5\text{-C}_5\text{H}_5)\text{Mn}(\text{CO})_2(\text{THF})$, $(\eta^5\text{-C}_5\text{R}'_5)\text{Mn}(\text{CO})_3$, and diazoalkanes. This surprising reaction was proposed to occur by direct transfer of a carbene to a bound carbonyl ligand. This work reports investigation of reaction 1 using $[\text{Cr}(\text{CO})_3(\text{C}_5\text{R}_5)]_2$ (R = H, CH₃) instead of $\text{Co}_2(\text{CO})_8$. Compared to Co, the Cr complexes show a greater tendency to dissociate and yield reactive monomeric $17e^-$ radical species by homolytic cleavage of the weak Cr–Cr bond.⁷ An additional difference in the Cr system is the presence of the highly stable Cr≡Cr complexes $[\text{Cr}(\text{CO})_2(\text{C}_5\text{R}_5)]_2$ for which there is no known stable counterpart in cobalt carbonyl chemistry. Interestingly, the complex $\text{Cr}_2(\text{CO})_5(\text{C}_5\text{H}_5)_2$, which is the analogue of the often proposed intermediate $\text{Co}_2(\text{CO})_7$, does not appear to have been detected.

In recent years methods based on density functional theory (DFT) have had great impact on organotransition metal chemistry.^{8–16} For example, recent work on metal–metal bonded complexes of first row transition metals has yielded quantitative predictions regarding structure and stability.^{17–20} A recent DFT study of the diazo to ketene conversion²¹ is of direct relevance to this work. This paper reports the convergence of theory and experiment to study the mechanism of activation of a diazo compound by concerted attack of two metal radicals.

- (4) (a) Grotjahn, D. B.; Collins, L. S. B.; Wolpert, M.; Bikzhanova, G. A.; Lo, H. C.; Combs, D.; Hubbard, J. L. *J. Am. Chem. Soc.* **2001**, *123*, 8260. (b) Grotjahn, D. B.; Lo, H. C. *J. Am. Chem. Soc.* **1996**, *118*, 2097. (c) Urtel, H.; Bikzhanova, G. A.; Grotjahn, D. B.; Hofmann, P. *Organometallics* **2001**, *20*, 3938.
- (5) Grotjahn, D. B.; Bikzhanova, G. A.; Collins, L. S. B.; Concolino, T.; Lam, K. C.; Rheingold, A. L. *J. Am. Chem. Soc.* **2000**, *122*, 5222.
- (6) (a) Herrmann, W. A.; Plank, J. *Angew. Chem., Int. Ed. Engl.* **1978**, *17*, 525. (b) Herrmann, W. A.; Plank, J.; Ziegler, M. L.; Weidenhammer, K. *J. Am. Chem. Soc.* **1979**, *101*, 3133.
- (7) (a) Hoff, C. D. *Coord. Chem. Rev.* **2000**, *206*, 451. (b) Watkins, W. C.; Jaeger, T.; Kidd, C. E.; Fortier, S.; Baird, M. C.; Kiss, G.; Roper, G. C.; Hoff, C. D. *J. Am. Chem. Soc.* **1992**, *114*, 907. (c) McLain, S. J. *J. Am. Chem. Soc.* **1988**, *110*, 643. (d) Adams, R. D.; Collins, D. E.; Cotton, F. A. *J. Am. Chem. Soc.* **1974**, *96*, 749. (e) The value of 2.215 Å is the average of the two reported Cr–Cr, bond lengths of 2.200 and 2.230 Å reported for $[\text{Cr}(\text{CO})_2\text{Cp}]_2$: Curtis, M. D.; Butler, W. M. *J. Organomet. Chem.* **1978**, *155*, 131.
- (8) Ehlers, A. W.; Frenking, G. *J. Am. Chem. Soc.* **1994**, *116*, 1514.
- (9) Delly, B.; Wrinn, M.; Lüthi, H. P. *J. Chem. Phys.* **1994**, *100*, 5785.
- (10) Li, J.; Schreckenbach, G.; Ziegler, T. *J. Am. Chem. Soc.* **1995**, *117*, 486.
- (11) Jonas, V.; Thiel, W. *J. Chem. Phys.* **1995**, *102*, 8474.
- (12) Barckholtz, T. A.; Bursten, B. E. *J. Am. Chem. Soc.* **1998**, *120*, 1926.
- (13) Niu, S.; Hall, M. B. *Chem. Rev.* **2000**, *100*, 353.
- (14) Macchi, P.; Sironi, A. *Coord. Chem. Rev.* **2003**, *238*, 383.
- (15) Carreon, J.-L.; Harvey, J. N. *Phys. Chem. Chem. Phys.* **2006**, *8*, 93.
- (16) Bühl, M.; Kabrede, H. *J. Chem. Theory Comput.* **2006**, *2*, 1282.
- (17) Schaefer, H. F.; III; King, R. B. *Pure Appl. Chem.* **2001**, *73*, 1059.
- (18) King, R. B.; Xie, Y.; Schaefer, H. F.; Richardson, N.; Li, S. *Inorg. Chim. Acta* **2005**, *358*, 1442.
- (19) Wang, H.; Xie, Y.; King, R. B.; Schaefer, H. F., III. *Inorg. Chem.* **2006**, *45*, 10849.
- (20) Li, Q.-S.; Zhang, X.; Xie, Y.; King, R. B.; Schaefer, H. F. *J. Am. Chem. Soc.* **2007**, *129*, 3433.
- (21) Seres, B.; Fördös, E.; Ungvári, N.; Fortman, G. C.; Hoff, C. D.; Ungvári F.; Kégl, T. Unpublished work.

2. Experimental

2.1. General Procedures. Unless stated otherwise, all operations were performed in a Vacuum Atmospheres glovebox under an atmosphere of purified argon or utilizing standard Schlenk tube techniques under argon. Toluene and THF were purified by distillation under argon from sodium benzophenone ketyl into flame dried glassware. $[\text{Cr}(\text{CO})_3(\text{C}_5\text{R}_5)]_2$ was prepared as described in earlier publications.⁷ Solutions of $\text{N}=\text{N}=\text{CHSiMe}_3$ (2.0 M in hexanes) were obtained from Sigma-Aldrich and used without further purification. FTIR data were obtained on a Perkin-Elmer system 2000 spectrometer. FTIR spectra for kinetic measurements were taken using a closed system FTIR cell that has been described in previous publications.²² NMR spectra were obtained on a Bruker AVANCE 500 MHz spectrometer. Electron spin resonance (ESR) spectra were taken with a Bruker EMX ESR Spectrometer.

Qualitative Studies of Reaction of $[\text{Cr}(\text{CO})_3(\text{C}_5\text{R}_5)]_2$ (R = H, Me) and $\text{N}_2\text{CHSiMe}_3$. Qualitative studies of reactions of $[\text{Cr}(\text{CO})_3(\text{C}_5\text{R}_5)]_2$ (R = H, CH₃) and $\text{N}_2\text{CHSiMe}_3$ were performed using standard Schlenk techniques. Reaction products were analyzed in terms of the bands shown in the Supporting Information Table ST-1 for the known complexes utilized. Approximate percent conversions were made on the basis of band-shape analysis using standard procedures.

Kinetic Studies of Reaction of $[\text{Cr}(\text{CO})_3(\text{C}_5\text{R}_5)]_2$ (R = H, Me) and $\text{N}_2\text{CHSiMe}_3$ under Low Pressures of Ar, CO, and N_2 . In a typical procedure, a solution of 0.1360 g $[\text{Cr}(\text{CO})_3(\text{C}_5\text{Me}_5)]_2$ in 15 mL of toluene was prepared in a Schlenk tube under argon to make a 0.0167 M solution (0.0334 M solution in radical). The Cr radical solution was then stirred for about 20 min to allow the compound to dissolve completely. In the glovebox the solution was loaded into a Hamilton gastight syringe fitted with a syringe filter. Outside the glovebox the $[\text{Cr}(\text{CO})_3(\text{C}_5\text{Me}_5)]_2$ solution was filtered into the closed system IR cell via syringe. The cell had been previously placed under an atmosphere of 9 psi of CO. The sample was shaken vigorously to ensure that the maximum amount of CO was dissolved into the solution. The IR cell was then attached to a constant temperature bath and allowed to reach thermal equilibrium at 298 K. The initial IR spectrum was then taken. A Hamilton gastight syringe was filled with 0.125 mL of a 2.0 M solution of $\text{N}_2\text{CHSiMe}_3$ in hexanes. Simultaneously the diazo solution was added and the timer was started. The sample was then shaken vigorously to ensure thorough mixing. IR spectra were taken on an average of every 60 s. Similar procedures were used to study the reaction of $[\text{Cr}(\text{CO})_3(\text{C}_5\text{R}_5)]_2$ (R = H, Me) and $\text{N}_2\text{CHSiMe}_3$ over a range of temperatures ($T = 278\text{--}308$ K) and pressures of Ar, CO, and N_2 ($p = 1\text{--}4.5$ atm).

Kinetic Studies of Reaction of $[\text{Cr}(\text{CO})_3(\text{C}_5\text{Me}_5)]_2$ and $\text{N}_2\text{CHSiMe}_3$ at 12.7 atm CO. In a typical procedure, a solution of 0.1936 g $[\text{Cr}(\text{CO})_3(\text{C}_5\text{Me}_5)]_2$ in 20 mL toluene was prepared in a Schlenk tube under argon to make a 0.0179 M solution. The solution was then mixed for about 20 min to allow the compound to dissolve. In the glovebox the solution was loaded into a Hamilton gastight syringe fitted with a syringe filter. Outside the glovebox the $[\text{Cr}(\text{CO})_3(\text{C}_5\text{Me}_5)]_2$ solution was filtered into the closed system IR cell via syringe using Schlenk techniques under Ar. The cell was then connected to a tank of CO. A Hamilton gastight syringe was used to add 0.180 mL of a 2.0 M solution of $\text{N}_2\text{CHSiMe}_3$ in hexanes to the cell after which the cell was immediately pressurized to a total of 173 psi. The reaction was thermostated at 290 K. IR spectra were taken as the reaction proceeded over the next week. Slow build up of the $\cdot\text{Cr}(\text{CO})_2(\text{ketene})\text{C}_5\text{Me}_5$ was monitored by IR peaks at 1672, 1908, and 1984 cm^{-1} . Other side-products that were seen during the course of the reaction include a slow buildup of both $\text{Cr}(\text{CO})_6$ (1981 cm^{-1}) and an unknown organic carbonyl near 1700 cm^{-1} which overlapped the broad band at 1670 cm^{-1} peak of the ketene complex.

- (22) Capps, K. B.; Bauer, A.; Sukcaroenphon, K.; Hoff, C. D. *Inorg. Chem.* **1999**, *38*, 6206.

ESR Measurements of the Reaction of $[\text{Cr}(\text{CO})_3(\text{C}_5\text{R}_5)_2]$ ($\text{R} = \text{H, Me}$) and $\text{Co}_2(\text{CO})_8$. In a representative experiment a 0.0162 M $[\text{Cr}(\text{CO})_3(\text{C}_5\text{R}_5)_2]$ ($\text{R} = \text{H, Me}$) solution was prepared under Schlenk techniques. The $[\text{Cr}(\text{CO})_3(\text{C}_5\text{R}_5)_2]$ solution (1.5 mL) was syringe filtered into a Pyrex NMR tube.²³ The end of the NMR tube was sealed and taken for ESR analysis. To the tube 0.5 equiv of $\text{N}_2\text{CH}(\text{SiMe}_3)$ (12 μL of 2.0 M in hexanes) was added. The tube was inverted several times to ensure proper mixing. The ESR spectrum was then taken. The reaction of $[\text{Cr}(\text{CO})_3(\text{C}_5\text{Me}_5)_2]$ with diazoalkane leads to an intense signal at $g = 2.007$. The reaction of $[\text{Cr}(\text{CO})_3(\text{C}_5\text{H}_5)_2]$ with diazoalkane leads to a small signal at $g = 2.005$. No signal was detected for the reaction of $\text{Co}_2(\text{CO})_8$ with the diazoalkane. Experimental conditions: T , 298 K; microwave power, 0.630 mW; microwave frequency, 9.840 GHz; modulation amplitude, 1.37 G.

Preparations of ^{13}C Labeled $[\text{Cr}(\text{CO})_3(\text{C}_5\text{R}_5)_2]$ ($\text{R} = \text{H, Me}$). In the glovebox 0.2146 g of $[\text{Cr}(\text{CO})_3(\text{C}_5\text{Me}_5)_2]$ was dissolved in 25 mL of toluene (0.016 M) with stirring for approximately 20 min. Using Schlenk techniques the solution was then syringe filtered into the closed system IR cell which in turn was pressurized to 230 psi with ^{13}C (99 atom % obtained from ISOTECH). CO exchange was allowed to occur overnight. The next morning the ^{13}C in the cell was evacuated and replaced by 193 psi of fresh ^{13}C . FTIR of the sample lead to the conclusion that this yielded approximately 96% $[\text{Cr}(^{13}\text{CO})_3(\text{C}_5\text{Me}_5)_2]$ with the remaining 4% primarily consisting of $[\text{Cr}(^{13}\text{CO})_2(^{12}\text{CO})(\text{C}_5\text{Me}_5)_2]$.

ESR of $[\text{Cr}(^{13}\text{CO})_3(\text{C}_5\text{R}_5)_2]$ ($\text{R} = \text{H, Me}$). In a representative experiment 1.5 mL of a 0.2146 M $[\text{Cr}(^{13}\text{CO})_3(\text{C}_5\text{Me}_5)_2]$ solution prepared as described above was syringe filtered into the a 5 mm pyrex NMR/ESR tube fitted with a screw cap and Teflon-coated silicone septum. The NMR/ESR tube had been purged with argon prior to addition. An ESR spectrum run prior to injection of $\text{N}_2\text{CHSiMe}_3$ showed no significant signal in keeping with the previously reported observation that in solution $^-\text{Cr}(\text{CO})_3(\text{C}_5\text{Me}_5)$ does not produce an observable ESR spectrum.²⁴ To the ESR tube 3.3 equiv of $\text{N}_2\text{CHSiMe}_3$ (20 μL of 2.0 M in hexanes) was added. The tube was inverted several times to ensure proper mixing, and the ESR spectrum was taken. As in the experiments with natural isotopic abundance complexes, the reaction of $[\text{Cr}(^{13}\text{CO})_3(\text{C}_5\text{Me}_5)_2]$ with diazoalkane led to an intense signal at $g = 2.007$ and the reaction of $[\text{Cr}(^{13}\text{CO})_3(\text{C}_5\text{H}_5)_2]$ with diazo led to a small signal at $g = 2.005$. An additional small signal seen in the spectrum for $[\text{Cr}(^{13}\text{CO})_3(\text{C}_5\text{H}_5)_2]$ was attributed to an unknown organic radical. Experimental conditions: T , 298 K; microwave power, 0.630 mW; microwave frequency, 9.807 GHz; modulation amplitude, 1.00 G.

NMR Studies of the Reaction of $[\text{Cr}(\text{CO})_3(\text{C}_5\text{H}_5)_2]$ and $\text{N}_2\text{CHSiMe}_3$. In a typical experiment 0.0321 g of $[\text{Cr}(\text{CO})_3(\text{C}_5\text{H}_5)_2]$ was dissolved in 5 mL C_6D_6 . One milliliter was then syringe filtered into an argon purged 5 mm Pyrex NMR tube fitted with a screw cap and septum. The sample was placed in the 500 MHz Bruker AVANCE 500 MHz NMR spectrometer. It was left in the NMR at 288 K for about 15 min to reach thermal equilibrium. The tube was then quickly ejected, loaded with 0.5 equiv of $\text{N}_2\text{CHSiMe}_3$ (12.0 μL of 2 M in hexanes), mixed, and placed back in the NMR. Spectra were run starting at about 240 s and successively run roughly every 80 s. In the Cp region (3.0–6.0 ppm) the only significant peak detected was a signal at ~ 4.21 ppm attributed to $[\text{Cr}(\text{CO})_2\text{C}_5\text{H}_5]_2$ which grew steadily during the course of the reaction. The reaction was confirmed by the FTIR spectra that were taken following the conclusion of the NMR experiment. The contents of the final solution included OCCHSiMe_3 (2107 cm^{-1}), traces of unreacted $[\text{Cr}(\text{CO})_3(\text{C}_5\text{H}_5)_2]$ (2009, 1946, 1920 cm^{-1}), and $[\text{Cr}(\text{CO})_2(\text{C}_5\text{H}_5)_2]$ (1901, 1878 cm^{-1}). NMR spectra were referenced to C_6HD_5 in the C_6D_6 at 7.15 ppm.

Calvet Calorimetric Measurement of Heat of Reaction of $[\text{Cr}_2(\text{CO})_2(\text{C}_5\text{H}_5)_2]$ and $[\text{Cr}(\text{CO})_3(\text{C}_5\text{H}_5)_2]$ with 1% Na/Hg. These experiments represent a modification of experimental procedures used in a previous report on enthalpies of reduction of organometallic compounds.²⁵ In the glovebox 0.5 mL of 1% Na/Hg was loaded into the cell of the Setaram-C-80 Calvet microcalorimeter under an atmosphere of CO. Subsequently added to the cell was 4.5 mL of THF that had been shaken and stored in the glovebox over the 1% Na/Hg and under a CO atmosphere. The solid-containing compartment of the calorimeter was loaded with 0.0132 g of $[\text{Cr}(\text{CO})_2(\text{C}_5\text{H}_5)_2]$ which had been recently recrystallized from heptane and methylene chloride. The calorimeter cell was assembled and sealed under a CO atmosphere and taken from the glovebox and loaded into the calorimeter. After reaching temperature equilibration the reaction was initiated. The thermogram indicated a rapid reaction which returned cleanly to baseline with no thermal signal indicative of any substantial secondary reactions occurring.

Following return to baseline, the cell was taken back into the glovebox. A sample analyzed by FTIR spectroscopy showed the presence of $\text{Na}^+[\text{Cr}(\text{CO})_3(\text{C}_5\text{H}_5)]^-$ as the sole organometallic product. The calorimetric signal was integrated and the average value for reduction of solid $[\text{Cr}(\text{CO})_2(\text{C}_5\text{H}_5)_2]$ to yield a THF solution of $\text{Na}^+[\text{Cr}(\text{CO})_3(\text{C}_5\text{H}_5)]^-$ was -94.6 ± 0.75 kcal mol^{-1} . The above procedure was also followed for the reaction of $[\text{Cr}(\text{CO})_3(\text{C}_5\text{H}_5)_2]$ with 1% Na/Hg. An average value of -80.7 ± 1.3 kcal mol^{-1} was obtained for the reduction of this solid to $\text{Na}^+[\text{Cr}(\text{CO})_3(\text{C}_5\text{H}_5)]^-$ in THF solution. Spectral data for the formation of $\text{Na}^+[\text{Cr}(\text{CO})_3(\text{C}_5\text{H}_5)]^-$ were identical for reductions starting from solid $[\text{Cr}(\text{CO})_2(\text{C}_5\text{H}_5)_2]$ and $[\text{Cr}(\text{CO})_3(\text{C}_5\text{H}_5)_2]$. Heats of solution for both complexes are assumed to be very similar. Spectral data for all relevant compounds are listed in the Supporting Information Table ST-1.

CO Exchange of $[\text{Cr}(\text{CO})_2(\text{C}_5\text{H}_5)_2]$ with ^{13}C . Under Schlenk techniques 0.055 mmol of $[\text{Cr}(\text{CO})_2(\text{C}_5\text{H}_5)_2]$ was dissolved in 10 mL of toluene. Under argon the solution was then transferred to the closed system FTIR cell via Hamilton gastight syringe. An initial FTIR spectrum was taken. The cell was then pressurized to 112 psi of ^{13}C and thermostated at 295 K for 1 h. No change was observed. In addition the temperature was increased from 295 to 310 K for an hour and finally to 323 K for 2 h. No significant change was seen. The sample was left at room temperature overnight and again no significant change was seen.

2.2. Theoretical Methods. Two DFT methods were used in this study. The first functional was the B3LYP method, which is a hybrid HF/DFT method using the combination of the three-parameter Becke functional (B3) with the Lee–Yang–Parr (LYP) generalized gradient correlation functional.^{26,27} The other DFT method used in the present paper was BP86, which combines Becke's 1988 exchange functional (B) with Perdew's 1986 gradient corrected correlation functional method (P86).^{28,29} It has been noted elsewhere that the BP86 method may be somewhat more reliable than B3LYP for the type of organometallic systems considered in this paper.^{30–32} In the present study, the B3LYP

- (23) Initial studies were made using quartz ESR tubes. It was found that a 5 mm screw cap NMR tube fitted with a teflon coated silicone septum showed no significant signal that overlapped with the signal for the Cr complex for these concentrated solutions.
 (24) Morton, J. R.; Preston, K. F.; Cooley, N. A.; Baird, M. C.; Krusic, P. J.; McLain, S. J. *J. Chem. Soc., Faraday Trans. 1* **1987**, *12*, 3535.

- (25) (a) Data obtained here for reduction of $\text{Cr}_2(\text{CO})_6(\text{C}_5\text{H}_5)_2$ using Na/Hg in THF under CO was found to be similar to previous measurements of the same reaction under Ar. Initial attempts at measuring the enthalpy of reduction utilized $\text{Na}^+\text{benzophenone}^-$ as has been described previously (ref 25b). During the course of these investigations it was found that because of pinacol coupling-type reactions that occur in some systems involving $\text{Na}^+\text{benzophenone}^-$ the Na/Hg reactions are more accurate. The purpose of the current work was to generate reliable enthalpies of reduction for $\text{Cr}_2(\text{CO})_6(\text{C}_5\text{H}_5)_2$. To the authors' knowledge the reaction itself has not been previously reported. Reduction of $\text{Cr}_2(\text{CO})_6(\text{C}_5\text{H}_5)_2$ ($n = 2, 3$) was measured by both methods $\text{Na}^+\text{benzophenone}^-$ and Na/Hg reduction. The differences between enthalpies of reduction (for $n = 2, 3$) were similar. Owing to pinacol coupling-like reactions only the Na/Hg measurements are considered reliable and reported here. Additional work on enthalpies of reduction are in progress and will be reported separately. (b) Kiss, G.; Nolan, S. P.; Hoff, C. D. *Inorg. Chim. Acta* **1994**, *227*, 285.
 (26) Becke, A. D. *J. Chem. Phys.* **1993**, *98*, 5648.
 (27) Lee, C.; Yang, W.; Parr, R. G. *Phys. Rev. B* **1988**, *37*, 785.
 (28) Becke, A. D. *Phys. Rev. A* **1988**, *38*, 3098.
 (29) Perdew, J. P. *Phys. Rev. B* **1986**, *33*, 8822.
 (30) Furche, F.; Perdew, J. P. *J. Chem. Phys.* **2006**, *124*, 044103.

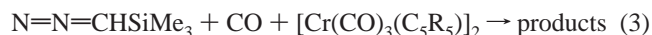
and BP86 methods agree with each other fairly well in predicting the structural characteristics of the $\text{Cp}_2\text{Cr}_2(\text{CO})_n$ (the common abbreviations $\text{Cp} = \text{C}_5\text{H}_5$ and $\text{Cp}^* = \text{C}_5\text{Me}_5$ will be used interchangeably) derivatives of interest. Although both the B3LYP and BP86 results are shown in the figures and tables, unless specifically noted, only the BP86 results (geometries, energies, and vibrational frequencies) are discussed in the text.

All calculations were performed using the double- ζ plus polarization (DZP) basis sets. The DZP basis sets used for carbon and oxygen add one set of pure spherical harmonic d functions with orbital exponents $\alpha_d(\text{C}) = 0.75$ and $\alpha_d(\text{O}) = 0.85$ to the standard Huzinaga–Dunning contracted DZ sets^{33,34} and are designated (9s5p1d/4s2p1d). For hydrogen, a set of p polarization functions $\alpha_p(\text{H}) = 0.75$ is added to the Huzinaga–Dunning DZ set. The loosely contracted DZP basis set for chromium is the Wachters primitive set³⁵ augmented by two sets of p functions and a set of d functions, contracted following Hood, Pitzer, and Schaefer,³⁶ designated (14s11p6d/10s8p3d).

The geometries of all structures were fully optimized using the DZP B3LYP and DZP BP86 methods, and the vibrational frequencies were determined by evaluating analytically the second derivatives of the energy with respect to the nuclear coordinates. The corresponding infrared intensities were also evaluated analytically. All of the computations were carried out with the Gaussian 03 program,³⁷ exercising the fine grid option (75 radial shells, 302 angular points) for evaluating integrals numerically, while the tight (10–8 hartree) designation is the default for the self-consistent field (SCF) convergence.

3. Results and Discussion

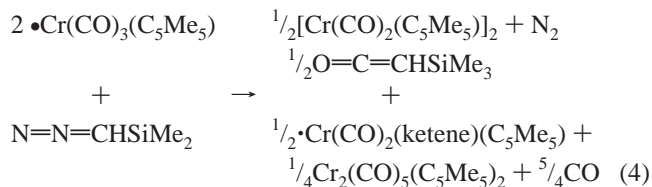
3.1. Qualitative and Kinetic Studies. Reaction 3 presented a number of surprises as well as difficulties in its study:



The yield and nature of the products were found to depend on the concentration of virtually every reactant and product in the equation.³⁸ Furthermore, the precursor complexes $[\text{Cr}(\text{CO})_3(\text{C}_5\text{R}_5)]_2$ ($\text{R} = \text{H}, \text{CH}_3$) dissociate to radicals to varying degrees depending on the temperature and R group. The third-order rate laws often found⁷ for $\cdot\text{Cr}(\text{CO})_3(\text{C}_5\text{Me}_5)$ also implicate a strong dependence on the absolute concentration of the metal. This section summarizes key aspects of this reaction studied under conditions designed to simplify and isolate given types of reactivity. The focus is on the reactions that occur at relatively high concentrations³⁸ (typically from 1 to 20 mM) of metal complex and ratios of Cr/diazo of 2/1 and 1/1, under CO, Ar, and N_2 atmospheres.

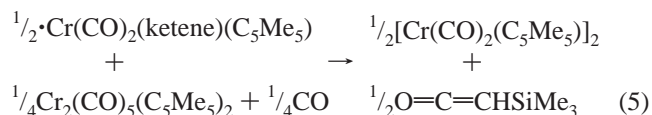
3.1.1. Reaction of $2\cdot\text{Cr}(\text{CO})_3(\text{C}_5\text{Me}_5)$ and NNCHSiMe_3 under Ar or N_2 . With a 2/1 Cr/diazoalkane mole ratio under Ar or N_2 , the reaction is best viewed as occurring in two stages.

The observed reactivity during “stage one”³⁹ corresponds roughly to the approximate stoichiometry shown in eq 4 below:



During this phase of the reaction, as shown in Figure 1, most of the chromium radical reacts and produces ketene and the $\text{Cr}=\text{Cr}$ triple-bonded product $\text{Cr}_2(\text{CO})_4(\text{C}_5\text{Me}_5)_2$ as well as intermediate products. Infrared bands assigned to the two proposed intermediate complexes $\cdot\text{Cr}(\text{CO})_2(\text{ketene})(\text{C}_5\text{Me}_5)$ and $\text{Cr}_2(\text{CO})_5(\text{C}_5\text{Me}_5)_2$ are observed to increase during this first stage of the reaction

During the second stage of the reaction, bands assigned to the two intermediate complexes are observed to decay according to the approximate stoichiometry shown in



Spectroscopic data during the later stage of reaction is shown in Supporting Information Figure S1. During this time the bands assigned to intermediates have reached a maximum and begin to decay liberating additional ketene and produce additional triple-bonded product. The clean nature of the reaction under these conditions is shown by the presence of an isosbestic point as shown in Supporting Information Figure S2. The fact that a significant amount of free ketene is liberated during this phase, in spite of low levels of free diazo present in solution, indicates that at least one of the intermediates contains a bound form of ketene or a precursor to it. Reactions performed under an N_2 atmosphere were studied in an attempt to see if either rate or product distribution differed significantly from reactions under Ar atmosphere. No real differences were observed implying that reversible dissociation of N_2 was not a rate determining step in the overall mechanism.

3.1.2. Reaction of $2\cdot\text{Cr}(\text{CO})_3(\text{C}_5\text{Me}_5)$ and NNCHSiMe_3 under CO. Reaction of $2\cdot\text{Cr}(\text{CO})_3(\text{C}_5\text{Me}_5)$ and $\text{N}=\text{N}=\text{CHSiMe}_3$ under CO at 1.6 atm CO pressure showed several distinctive differences compared to reaction under argon. The first is a markedly slower rate of reaction. The second is that less $[\text{Cr}(\text{CO})_2(\text{C}_5\text{Me}_5)]_2$ is produced and less $\cdot\text{Cr}(\text{CO})_3(\text{C}_5\text{Me}_5)$ is consumed during ketene production. This implies that it is CO gas that is utilized to produce ketene rather than the organometallic complex being decarbonylated by the diazoalkane. In addition, the level of detectable intermediates under CO at a 2/1 Cr/diazoalkane mole ratio is lower than what is observed under argon. Finally, as shown in Figure 2 the reaction shows a characteristic “S” shape curve for production of ketene, consistent with an induction period followed by a relatively rapid

(31) Wang, H. Y.; Xie, Y.; King, R. B.; Schaefer, H. F. *J. Am. Chem. Soc.* **2005**, *127*, 11646.

(32) Wang, H. Y.; Xie, Y.; King, R. B.; Schaefer, H. F. *J. Am. Chem. Soc.* **2006**, *128*, 11376.

(33) Dunning, T. H. *J. Chem. Phys.* **1970**, *53*, 2823.

(34) Huzinaga, S. *J. Chem. Phys.* **1965**, *42*, 1293.

(35) Wachters, A. J. H. *J. Chem. Phys.* **1970**, *52*, 1033.

(36) Hood, D. M.; Pitzer, R. M.; Schaefer, H. F. *J. Chem. Phys.* **1979**, *71*, 705.

(37) Frisch, M. J.; et al. *Gaussian 03*, revision C 02; Gaussian, Inc.: Wallingford, CT, 2004.

(38) Several intermediate complexes are either detected or proposed to be present in reactions studied at relatively low concentrations of diazoalkane. Attempts to extend these studies to regimes of high diazoalkane concentration produced unknown products. It seems plausible that these resulted from radical intermediates already containing a bound diazoalkane or ketene moiety reacting further with additional equivalents of free diazoalkane to produce oligomeric products. Catalytic conversion of diazoalkane to ketene could be achieved by repeated injections of small amounts of diazoalkane. However “flooding” the system with a high concentration of diazoalkane was found to produce side products of unknown and presumably oligomeric nature.

(39) Separation of the reaction into two phases is somewhat artificial and is meant to show the qualitative nature of the two periods. In the first phase intermediates build up and in the second they decay. In terms of reaction kinetics there is of course one continuous process and, particularly in the middle where the “two phases” overlap, there is no clear distinction. Nevertheless the very beginning and ending parts of the reaction approach the limiting stoichiometries discussed.

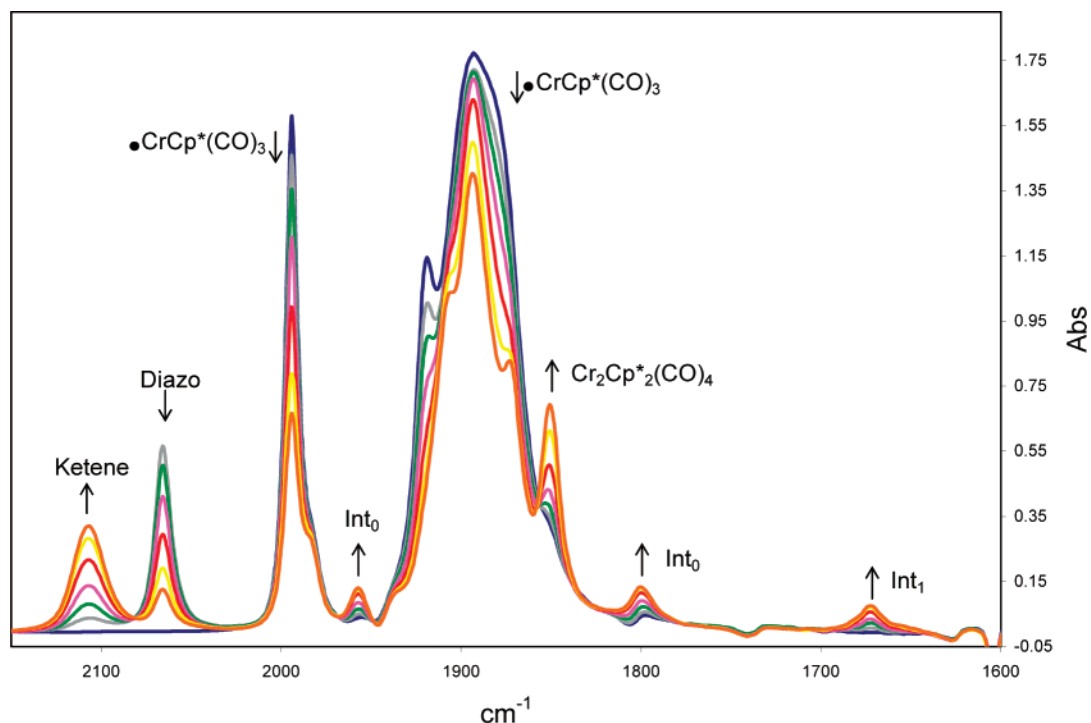


Figure 1. FTIR spectral data during initial stage of reaction of $\cdot\text{Cr}(\text{CO})_3(\text{C}_5\text{Me}_5)$ (~ 0.033 M) with $\text{N}=\text{N}=\text{CHSiMe}_3$ (~ 0.0165 M) at 25°C in toluene under an argon atmosphere. Bands assigned to $\text{int}_0 = \text{Cr}_2(\text{CO})_5(\text{C}_5\text{Me}_5)_2$ are at 1957 , 1894 , and 1799 cm^{-1} and bands assigned to $\text{int}_1 = \cdot\text{Cr}(\text{CO})_2(\text{ketene})(\text{C}_5\text{Me}_5)$ occur at 1984 , 1908 , and 1672 cm^{-1} . In the text and figures the common abbreviations $\text{Cp} = \text{C}_5\text{H}_5$ and $\text{Cp}^* = \text{C}_5\text{Me}_5$ are used interchangeably. For complete band assignments see Table ST-1.

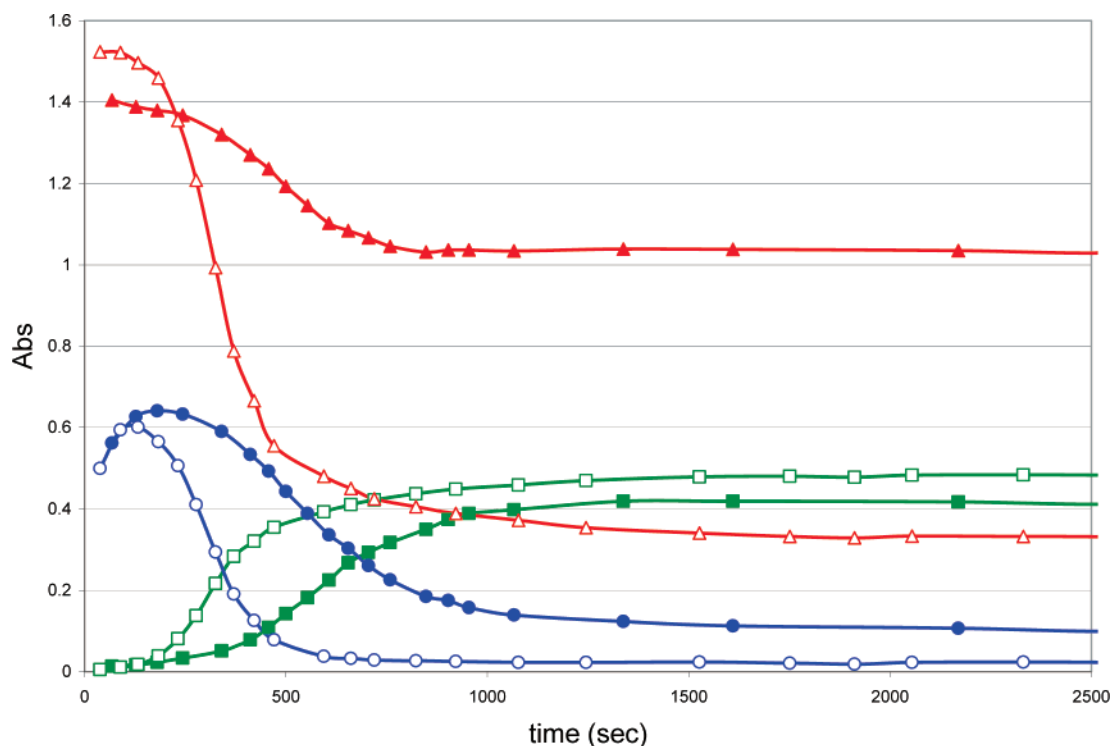


Figure 2. Absorbance versus time plots for key species in reaction of $\cdot\text{Cr}(\text{CO})_3(\text{C}_5\text{Me}_5)$ (~ 0.033 M) with $\text{N}=\text{N}=\text{CHSiMe}_3$ (~ 0.0165 M) at 25°C in toluene under Ar and CO at 1.6 atm of pressure. Absorbance bands used for quantification of key species: $\text{N}_2\text{CHSiMe}_3 = 2066$ cm^{-1} ; $\text{OCCHSiMe}_3 = 2107$ cm^{-1} ; $\cdot\text{Cr}(\text{CO})_3(\text{C}_5\text{Me}_5) = 1994$ cm^{-1} ; ●, $\text{N}_2\text{CHSiMe}_3$ (CO); ○, $\text{N}_2\text{CHSiMe}_3$ (Ar); ■, OCCHSiMe_3 (CO); □, OCCHSiMe_3 (CO); ▲, $\cdot\text{Cr}(\text{CO})_3(\text{C}_5\text{Me}_5)$ (CO); △, $\cdot\text{Cr}(\text{CO})_3(\text{C}_5\text{Me}_5)$ (Ar).

reaction. The “S” shape is more pronounced under Ar atmosphere compared to CO.

3.1.3. Reaction of $\cdot\text{Cr}(\text{CO})_3(\text{C}_5\text{Me}_5)$ and $\cdot\text{Cr}^{13}\text{CO}_3(\text{C}_5\text{Me}_5)$ with NNCHSiMe_3 , FTIR and ESR Studies. Reaction of $\cdot\text{Cr}(\text{CO})_3(\text{C}_5\text{Me}_5)$ with $\text{N}=\text{N}=\text{CHSiMe}_3$ in a 1/1 ratio was

found to show significant differences from those studied at a 2/1 molar ratio. This is presumably because the reductive elimination step is dinuclear and the presence of excess diazo in solution generates $\cdot\text{Cr}(\text{CO})_2(\text{ketene})(\text{C}_5\text{Me}_5)$ more quickly than it is consumed. In addition it was found that under a CO

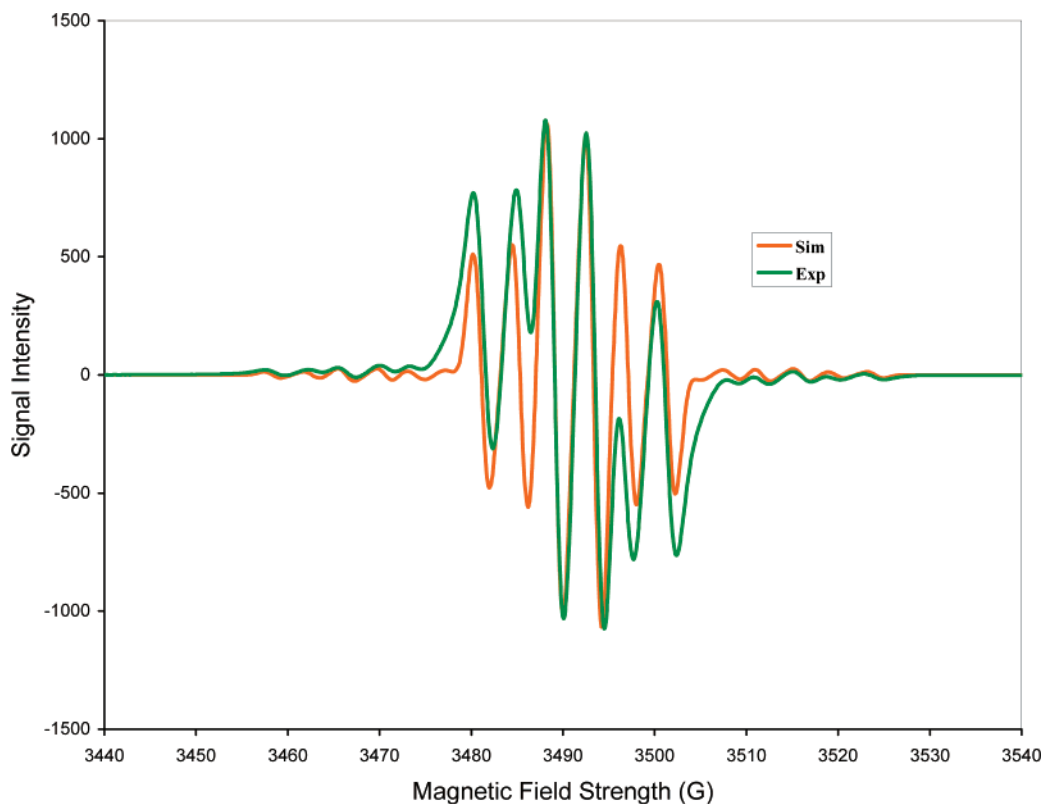
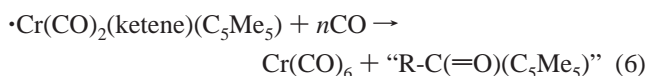


Figure 3. Experimental and simulated room-temperature X-band (9.807 GHz) ESR spectra for $\cdot\text{Cr}^{(13}\text{CO})_2(\eta^2\text{-O}=\text{}^{13}\text{C}=\text{CHSiMe}_3)(\text{C}_5\text{Me}_5)$. Simulated data are fit assuming 95% isotopic substitution in ^{13}C and natural abundance in ^{53}Cr and the following parameters: $g(\text{iso}) = 2.007$; $A(^{53}\text{Cr}) = 42.5$ MHz; $A(^{13}\text{C } a)_2 = 22.5$ MHz; $A(^{13}\text{C } b)_1 = 12.0$ MHz; 3 MHz Gaussian line widths. Experimental and simulated ESR spectra for natural isotopic abundance $\cdot\text{Cr}(\text{CO})_2(\text{O}=\text{C}=\text{CHSiMe}_3)(\text{C}_5\text{Me}_5)$ are shown in Figure S3 and exhibit hyperfine splitting only from ^{53}Cr .

atmosphere⁴⁰ the intermediate complex $\text{Cr}_2(\text{CO})_5(\text{C}_5\text{Me}_5)_2$ is carbonylated but $\cdot\text{Cr}(\text{CO})_2(\text{ketene})(\text{C}_5\text{Me}_5)$ reacts only extremely slowly with CO. The net result is that significant quantities of the radical ketene complex buildup. This increase can be seen in both the IR and ESR spectra.

FTIR studies of the reaction of $\cdot\text{Cr}(\text{CO})_3(\text{C}_5\text{Me}_5)$ with $\text{N}=\text{N}=\text{CHSiMe}_3$ at a 1/1 molar ratio were studied under CO pressures of 10–700 psi. Under higher pressures the reaction is slow and may take up to a week to go to completion at room temperature. The principal product under these conditions is the intermediate complex formulated as $\cdot\text{Cr}(\text{CO})_2(\text{ketene})(\text{C}_5\text{Me}_5)$. Attempts to obtain crystals of this highly air-sensitive complex were unsuccessful despite repeated attempts. During these long reactions under high CO pressure, slow buildup of $\text{Cr}(\text{CO})_6$, identified by its characteristic IR spectrum, and an unknown organic carbonyl compound were observed to be formed, presumably from⁴¹



The formulation of the intermediate as $\cdot\text{Cr}(\text{CO})_2(\text{ketene})(\text{C}_5\text{Me}_5)$ is based on its vibrational spectrum (Table ST-1) and observed release of ketene upon reaction with $\cdot\text{Cr}(\text{CO})_3(\text{C}_5\text{Me}_5)$ or $\text{Cr}_2(\text{CO})_5\text{Cp}^*_2$ as well as ESR spectroscopy. Study of the

(40) In addition to external gas pressure utilized in the reaction, the shape of the reaction container and how it is stirred can also play a role in terms of how quickly any CO released in solution can escape to the gas phase. In the narrow confines of a sealed ESR tube, for example, even reactions run initially under argon may soon buildup significant CO concentrations serving to quench the reaction as well as alter the product distribution. For that reason ESR studies described are primarily qualitative in nature.

reactions of $\cdot\text{Cr}(\text{CO})_3(\text{C}_5\text{R}_5)$ ($\text{R} = \text{H}, \text{CH}_3$) with NNCHSiMe_3 by ESR spectroscopy showed the presence of radical species that build up and decay in rough accord with the FTIR spectroscopic studies discussed above. Representative spectroscopic data illustrating the buildup and slow decay of this complex as well as the spectrum of the natural isotope abundance species are shown in Supporting Information Figure S3.

Reaction studies using analogous ESR techniques to those shown for $\cdot\text{Cr}(\text{CO})_3(\text{C}_5\text{Me}_5)$ were also performed for reactions of $\cdot\text{Cr}(\text{CO})_3(\text{C}_5\text{H}_5)$ and $\text{Co}_2(\text{CO})_8$. As shown in Supporting Information Figure S4 the overall level of radical concentration is approximately 10 times lower for the Cp compared to the Cp^* chromium systems. The reaction of $\text{Co}_2(\text{CO})_8$ with diazo showed no detectable signal above background noise. Radical species in the cobalt system were estimated to be present at levels at least 6 orders of magnitude lower than for the chromium systems under comparable conditions.

The ^{13}CO labeled radical $\cdot\text{Cr}^{(13}\text{CO})_3(\text{C}_5\text{Me}_5)$ complex was prepared and allowed to react with $\text{N}=\text{N}=\text{CHSiMe}_3$ to prepare in situ the isotopically labeled complex $\cdot\text{Cr}^{(13}\text{CO})_2(\eta^2\text{-O}=\text{}^{13}\text{C}=\text{CHSiMe}_3)(\text{C}_5\text{Me}_5)$. ESR spectra for this complex and a com-

(41) (a) Production of $\text{Mo}(\text{CO})_6$ from $\text{RMo}(\text{CO})_5\text{C}_5\text{R}_5$ under CO pressure has been shown to yield $\text{R}-\text{C(=O)}-\text{C}_5\text{R}_5$ as described in ref 41b. The complex $\cdot\text{Cr}(\text{CO})_2(\eta^2\text{-ketene})(\text{C}_5\text{Me}_5)$ is resistant to carbonylation. It seems possible that this is due to an unfavorable pre-equilibrium to generate $\cdot\text{Cr}(\text{CO})_3(\eta^1\text{-ketene})(\text{C}_5\text{Me}_5)$. Once formed, this radical complex, rather than liberate ketene may form a C–C bonded complex in which the (η^1 -ketene) moiety migrates to the cyclopentadienyl ring and then adds further CO yielding ultimately $\text{Cr}(\text{CO})_6$ and some complex organic carbonyl. The growth of a broad band near 1700 cm^{-1} in these experiments is in keeping with that hypothesis but no attempt was made to further characterize this side product. (b) Nolan, S. P.; de la Vega, R. L.; Mukerjee, S. K.; Hoff, C. D. *Inorg. Chem.* **1986**, 25, 1160.

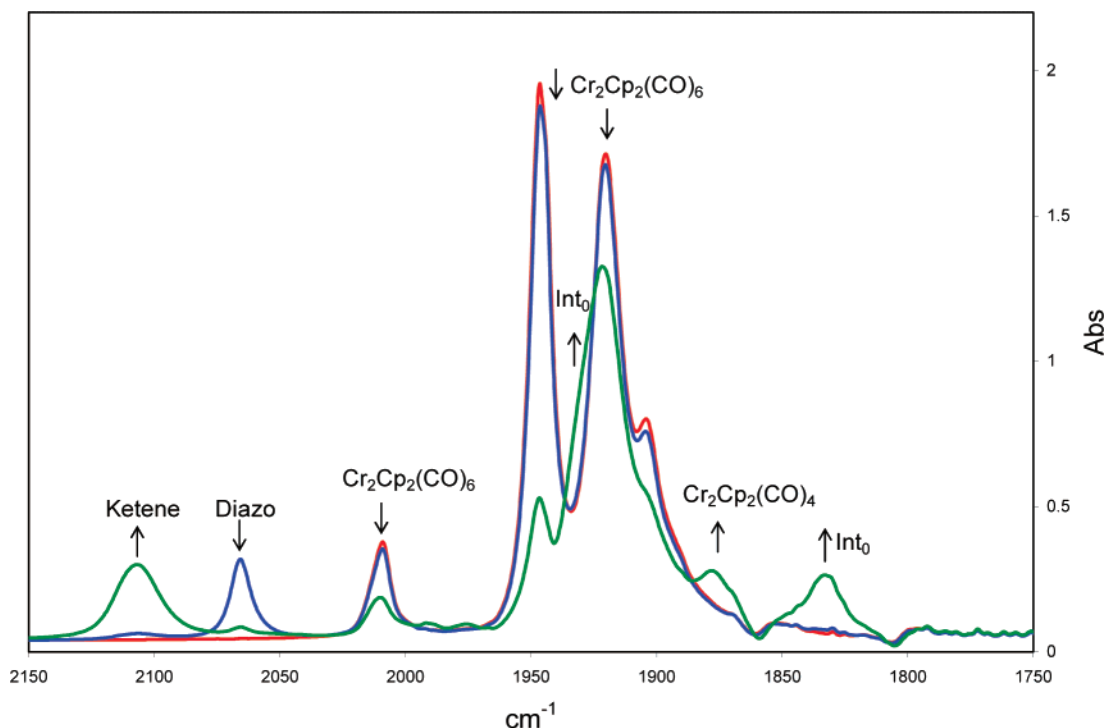


Figure 4. Stock solution of $[\text{Cr}(\text{CO})_3\text{Cp}]_2$ (0.0163 M) in toluene under argon prior to addition of NNCHSiMe_3 (0.0108 M) in a 1.5/1 molar ratio at 25 °C (red spectrum), $t \approx 30$ s following addition of NNCHSiMe_3 (blue spectrum) and $t \approx 60$ s (green spectrum). Little reaction occurs during the initial induction period as shown in the blue spectrum. The green spectrum shows rapid growth in free ketene, nearly complete reaction of initial diazo and $[\text{Cr}(\text{CO})_3\text{Cp}]_2$, minor buildup of $[\text{Cr}(\text{CO})_2\text{Cp}]_2$, and the presence of an intermediate complex. For band positions see Table ST-1.

puter simulation are shown in Figure 3. Both display a coupling to ^{13}C O not present in the natural abundance spectrum shown in Supporting Information Figure S3. The spectrum of the ^{13}C O labeled complex consists essentially of a triplet of doublets centered at $g = 2.007$, with low-intensity satellites due to ^{53}Cr ($I = 3/2$, 9.5% abundant). The largest hyperfine coupling is to the metal, $A(^{53}\text{Cr}) = 42.5$ MHz, with additional hyperfine splitting assigned as 22.5 MHz for the two equivalent ^{13}C O ligands and 12.0 MHz for $\eta^2\text{-O}=\text{C}=\text{CHSiMe}_3$. No hyperfine splitting is assignable to ^1H , as indicated by the simple ESR spectra of the natural abundance spectrum shown in Supporting Information Figure S3.

It cannot be excluded that low levels of other radical species may be present in solution, but the dominant pattern seen in a number of experiments was reproducible and the fit of computed and experimental data are good. The growth and decay of the peaks assigned to this intermediate as followed by ESR were also observed in FTIR studies done in parallel reactions.

These ESR results can be compared with those for other organochromium radicals.^{42,43} The value for isotropic ^{53}Cr hyperfine coupling, 42.5 MHz, is comparable, but larger than that seen for $\cdot\text{Cr}(\text{CO})_3(\text{C}_5\text{H}_5)$ ($a_{\text{iso}}(^{53}\text{Cr}) = 23$ MHz, based on measurements at low temperatures in doped single crystals of the diamagnetic host, $\text{CpMn}(\text{CO})_3$),^{43b} which indicates the

significant Cr(I) character of $\cdot\text{Cr}(\text{CO})_2(\eta^2\text{-O}=\text{C}=\text{CHSiMe}_3)(\text{C}_5\text{Me}_5)$. The complex $\cdot\text{Cr}(\text{CO})_3(\text{C}_5\text{H}_5)$ also exhibited hyperfine coupling from the carbonyl ligands (detected in natural isotopic abundance) with $a_{\text{iso}}(^{13}\text{C}) = 25$ MHz,^{43b} quite close to the value observed here (we are unaware of any relevant data for the ketene-based ^{13}C hyperfine coupling).

An interesting difference, however, is that the symmetrical parent radical, as well as related derivatives $\cdot\text{Cr}(\text{CO})_3(\text{C}_5\text{R}_5)$ ($\text{R} = \text{H}, \text{CH}_3, \text{Ph}$) are known to display *no* solution-phase ESR spectra at room temperature.⁴² However, for species of lower effective symmetry such as $\cdot\text{Cr}(\text{CO})_2(\text{L})(\text{C}_5\text{Me}_5)$,⁴³ $\cdot\text{Cr}(\text{CO})_2(\text{RC}\equiv\text{CR})(\text{C}_6\text{Me}_6)^+$,⁴⁴ and $\cdot\text{Cr}(\text{CO})_2(\eta^3\text{-tris}(\text{pyrazolyl})\text{borato})(\text{PMe}_3)$ ⁴⁵ solution-phase spectra are reported even at ambient temperature. These arguments support assignment of the radical species in solution as $\cdot\text{Cr}(\text{CO})_2(\eta^2\text{-O}=\text{C}=\text{CHSiMe}_3)(\text{C}_5\text{Me}_5)$, which likewise has lower effective symmetry. Computed SOMO and spin density data are shown in Supporting Information Figure S5 and also support a highly delocalized radical which is predominantly metal based. Similar conclusions⁴⁴ were made for the cationic acetylene complexes $\cdot\text{Cr}(\text{CO})_2(\text{RC}\equiv\text{CR})(\text{C}_6\text{Me}_6)^+$ which are probably closest in nature to the proposed intermediate ketene radical complex reported here.

Reaction of $\cdot\text{Cr}(\text{CO})_3(\text{C}_5\text{Me}_5)$ and $\text{N}=\text{N}=\text{CHSiMe}_3$ was also investigated by FTIR spectroscopy as shown in Supporting Information Figure S6. A shift in the assigned vibrational bands of all assigned bands was observed (see Supporting Information Table ST-1). However of principal interest was the shift in $\nu(\text{CO})$ of the assigned band of the coordinated ketene from 1672 to 1637 cm^{-1} for $\cdot\text{Cr}(\text{CO})_2(\eta^2\text{-O}=\text{C}=\text{CHSiMe}_3)(\text{C}_5\text{Me}_5)$.

(42) (a) Rieger, P. H. *Coord. Chem. Rev.* **1994**, *135/136*, 203. (b) Hoobler, R. J.; Hutton, M. A.; Dillard, M. M.; Castellani, M. P.; Rheingold, A. L.; Rieger, A. L.; Rieger, P. H.; Richards, T. C.; Geiger, W. E. *Organometallics* **1993**, *12*, 116. (c) Fortier, S.; Baird, M. C.; Preston, K. F.; Morton, J. R.; Ziegler, T.; Jaeger, T. J.; Watkins, C.; MacNeil, J. H.; Watson, K. A.; Hensel, K.; Page, Y. L.; Charland, J. P.; Williams, A. J. *J. Am. Chem. Soc.* **1991**, *113*, 542.

(43) (a) Cooley, N. A.; Baird, M. C.; Morton, J. F.; Preston, K. F.; Page, Y. L. *J. Magn. Res.* **1988**, *76*, 325. (b) Morton, J. R.; Preston, K. F.; Cooley, N. A.; Baird, M. C.; Krusic, P. J.; McLain, S. L. *J. Chem. Soc., Faraday Trans. 1* **1987**, *83*, 3535.

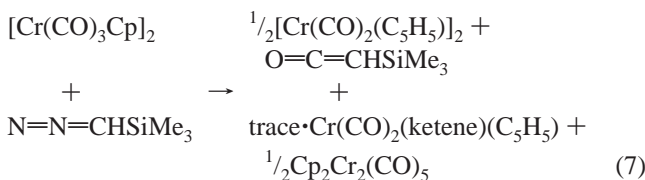
(44) Connelly, N. G.; Orpen, A. G.; Rieger, A. L.; Rieger, P. H.; Scott, C. J.; Rosair, G. M. *Chem. Commun.* **1992**, 1293.

(45) MacNeil, J. H.; Watkins, W. C.; Baird, M. C.; Preston, K. F. *Organometallics* **1992**, *11*, 2761.

This is strong evidence that loss of N₂ occurs previous to the formation of this intermediate.

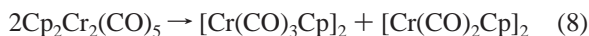
3.1.4. Reaction of [Cr(CO)₃(C₅H₅)₂] and NNCHSiMe₃. Reaction of [Cr(CO)₃Cp]₂ with N=N=CHSiMe₃ in a 1.5/1 stoichiometric ratio {a 3/1 ratio based on the monomeric radical •Cr(CO)₃(C₅H₅)} under argon was found to occur more rapidly for the C₅H₅ than the C₅Me₅ system. That rapid occurrence is despite the fact that lower concentrations of radical species are present in the Cp system. Production of ketene was nearly complete following a short induction period as shown in Figure 4. The initial organometallic products are a previously unknown intermediate complex with major bands near 1931 and 1833 cm⁻¹ and a minor band near 2006 cm⁻¹ as well as small quantities of the known triple-bonded complex [Cr(CO)₂Cp]₂. As discussed later, the ν(CO) frequencies are in good agreement with formulation of the previously unreported product as Cp₂Cr₂(CO)₅ on the basis of high level density functional theory.

Thus the first stage of the reaction of [Cr(CO)₃Cp]₂ with N=N=CHSiMe₃ is considered to occur in a manner similar to that for 2•Cr(CO)₃(C₅Me₅) but with only trace amounts of the bound ketene radical and a much greater amount of Cp₂Cr₂(CO)₅.

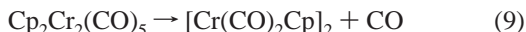


A very small band near 1700 cm⁻¹ can be detected and is assigned to small amounts of •Cr(CO)₂(ketene)(C₅H₅) by comparison with the band near 1672 cm⁻¹ assigned to •Cr(CO)₂(ketene)(C₅Me₅). In addition, ESR measurements for the Cp system show the presence of a rapidly decaying radical species in low concentration as discussed above. Reactions done with a greater excess of [Cr(CO)₃Cp]₂ such that the Cr/diazo mole ratio was 3/1 were found to produce the bands assigned to Cp₂Cr₂(CO)₅ more rapidly with the near absence of initially produced [Cr(CO)₂Cp]₂.

The second stage of reaction under an argon atmosphere as shown in Supporting Information Figure S7 was initially interpreted as a disproportionation reaction:



However decay of Cp₂Cr₂(CO)₅ is best described by



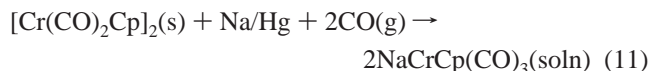
The product ratio observed in decomposition of Cp₂Cr₂(CO)₅ was found to depend on CO pressure. At high CO pressures predominantly [Cr(CO)₃Cp]₂ is produced, and at very low CO pressures [Cr(CO)₂Cp]₂ is the major product as shown in Supporting Information Figure S8.

Kinetic studies of the rate of decay of Cp₂Cr₂(CO)₅ as a function of temperature and CO pressure were performed. First-order plots of the rate of decay of Cp₂Cr₂(CO)₅ under argon as a function of temperature, producing primarily [Cr(CO)₂Cp]₂ are shown in Supporting Information Figure S9, and lead to estimated activation parameters of ΔH[‡] = 23 kcal mol⁻¹ and

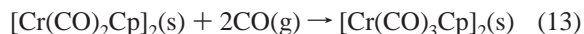
ΔS[‡] = 8 cal mol⁻¹ K⁻¹ for reaction 9. The product branching ratio between reactions 9 and 10 was observed to depend on CO pressure, but for a fixed CO pressure the selectivity showed little temperature variation among experiments done at 15, 25, and 35 °C. This implies a similar enthalpy of activation for both loss of CO as well as addition of CO to Cp₂Cr₂(CO)₅.

The relatively slow rate of reactions 9 and 10, as well as the DFT calculations discussed below, suggested that Cp₂Cr₂(CO)₅ might be a ground-state triplet, and as such not display a detectable NMR signal (nor ambient temperature ESR). The reaction of [Cr(CO)₃Cp]₂ with N=N=CHSiMe₃ was therefore studied by NMR spectroscopy in C₆D₆ at 15 °C. The first NMR spectrum was taken approximately 240 s after initiating reaction. At that time, complete conversion of the diazo to ketene had occurred, in keeping with earlier FTIR studies. A very small broad peak due to [Cr(CO)₃Cp]₂ was detected near 5.3 ppm and underwent only minor changes during the reaction. The only major change seen in the NMR spectra was the appearance “out of nowhere” of a steadily increasing signal near 4.2 ppm due to [Cr(CO)₂Cp]₂ as shown in Supporting Information Figure S10. These studies strongly support the formulation of the intermediate as ³Cp₂Cr₂(CO)₅.

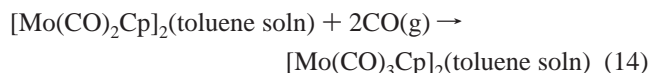
3.1.5. Calorimetric Study of Enthalpies of Reduction of [Cr(CO)₂Cp]₂ and [Cr(CO)₃Cp]₂ by Na/Hg under CO. To make an estimate of the Cr≡Cr bond strength in [Cr(CO)₂Cp]₂, the energies of reactions 11 [ΔE = -94.9 ± 0.8 kcal mol⁻¹] and 12 [ΔE = -80.7 ± 1.3 kcal mol⁻¹] were measured by solution calorimetry in THF solution.



The difference between reactions 11 and 12 yield a value for reaction 13 of ΔE = -14.2 ± 2.1 kcal mol⁻¹ since all other terms cancel.



The computed energy change is based on reactions of the solids as shown in eq 13. Conversion of the value for ΔE_{solids} to ΔH_{solns} however results in no significant change in the value of -14.2 kcal mol⁻¹ for the enthalpy of reaction 13 with all species in solution.⁴⁶ Previously we have reported⁴⁷ measurements of the enthalpy of reaction 14 ΔH = -40.3 kcal mol⁻¹:



The considerably more exothermic reaction of the Mo≡Mo complex as shown in reaction 14 is in keeping with its generally

(46) The value for the enthalpy of reaction 13 as measured from solid to solid should require little adjustment for reaction in toluene solution. Measurement of the enthalpy of solution of [Cr(CO)₃Cp]₂ presents problems owing to its dissociation to radicals. However experiments with the corresponding molybdenum complexes (which undergo no such dissociation) suggest that the enthalpy of solution of [Cr(CO)₃Cp]₂ in toluene is approximately 1.2 kcal mol⁻¹ more endothermic than for [Cr(CO)₂Cp]₂. However, the actual calorimetric measurements are for ΔE and not ΔH in the closed system. Since ΔH = ΔE + ΔPV, correction for the two moles of gas absorbed in the reaction (RTΔn of ~1.2 kcal mol⁻¹) will essentially cancel the difference in the estimated enthalpies of solution.

(47) Nolan, S. P.; de la Vega, R. L.; Hoff, C. D. *Inorg. Chem.* **1986**, *25*, 4446.

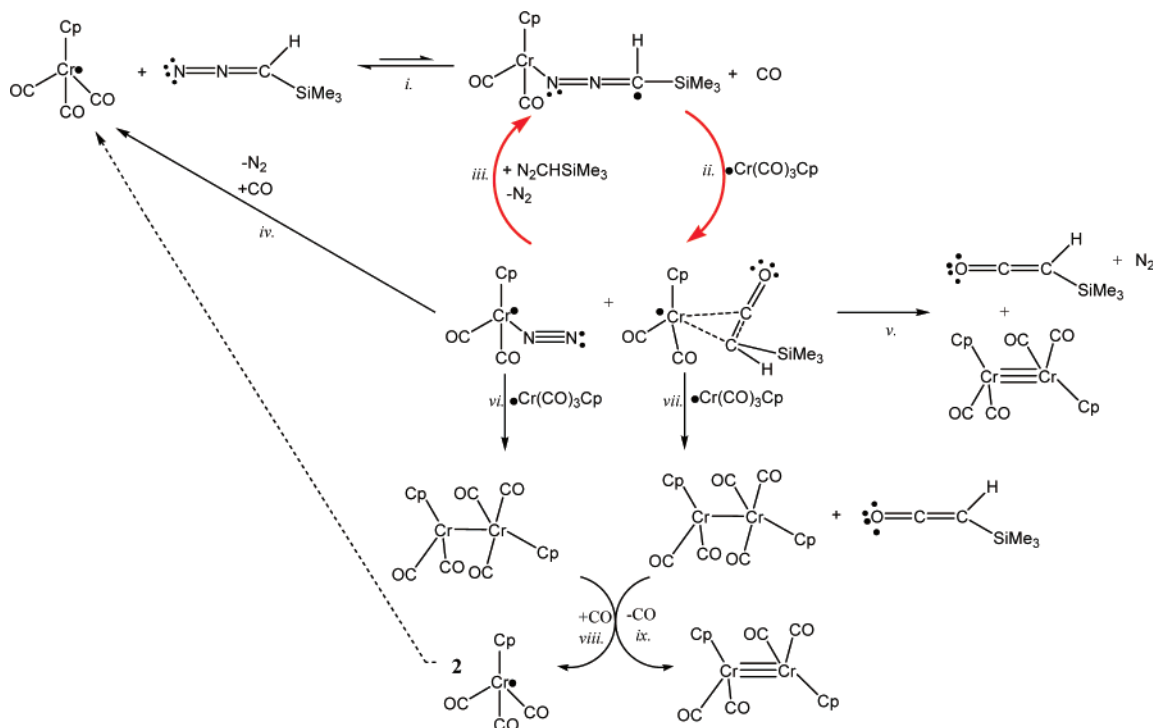


Figure 5. Proposed reaction scheme for reaction of $\cdot\text{Cr}(\text{CO})_3(\text{C}_5\text{Me}_5)$.

much greater reactivity compared to the relatively inert $\text{Cr}\equiv\text{Cr}$ complex.⁴⁸ The difference between the enthalpies of reactions 13 and 14 (ca. $-26 \text{ kcal mol}^{-1}$) implies that while the $\text{Cr}-\text{Cr}$ single bond is much weaker than the $\text{Mo}-\text{Mo}$ single bond, that situation does not extend to the triple-bonded complexes.⁴⁹

In fact, use of a value of $\text{Cr}-\text{CO} = 37 \text{ kcal mol}^{-1}$ ⁵⁰ leads to an estimate of the $\text{Cr}\equiv\text{Cr}$ bond strength of 74 kcal mol^{-1} , slightly larger than the previous reported estimate of the $\text{Mo}\equiv\text{Mo}$ bond strength of 69 kcal mol^{-1} .

3.1.6. Attempted ^{13}C O Exchange in $[\text{Cr}(\text{CO})_2\text{Cp}]_2$. Investigation as to the reversibility of reaction 9 showed that CO did not readily add at pressures up to $\sim 10 \text{ atm}$ at room temperature. Wrighton and co-workers have reported slow carbonylation at pressures in excess of 100 atm .⁵¹ That reaction involves the addition of 2 mol of CO presumably through intermediate $\text{Cp}_2\text{Cr}_2(\text{CO})_5$. To test this possibility, we studied reaction 15



At ^{13}CO pressure of $\sim 10 \text{ atm}$ and at temperatures up to $\sim 50 \text{ }^\circ\text{C}$ no real sign of incorporation of ^{13}CO label in $[\text{Cr}(\text{CO})_2\text{Cp}]_2$ was observed. This was taken to indicate little if

(48) Curtis, M. D. *Polyhedron* **1987**, *6*, 759.

(49) The $\text{Cr}-\text{Cr}$ single bond strength is on the order of 15 kcal mol^{-1} and the $\text{Mo}-\text{Mo}$ bond strength is on the order of $32.5 \text{ kcal mol}^{-1}$. This difference ($17.5 \text{ kcal mol}^{-1}$) alone would make the enthalpy of eq 14 exothermic by that amount. The $\text{Mo}-\text{CO}$ bond strength is typically viewed as being $\sim 4 \text{ kcal mol}^{-1}$ greater than the $\text{Cr}-\text{CO}$ bond strength. Since two CO bonds are transferred that would make an estimate of $\Delta H \cong -17.5 + 2 \times -4 = -25.5 \text{ kcal mol}^{-1}$. This is close to the measured difference and implies that the $\text{Cr}\equiv\text{Cr}$ and $\text{Mo}\equiv\text{Mo}$ bond strengths are roughly comparable in terms of the reaction: $\text{Cp}(\text{CO})_2\text{M}\equiv\text{M}(\text{CO})_2\text{Cp} \rightarrow 2\text{MCP}(\text{CO})_2$ as a definition of the bond dissociation energy (BDE) reaction. It is apparently the case that the weak nature of the $\text{Cr}-\text{Cr}$ single bond does not carry over to the triple bond, at least in comparison to corresponding Mo complexes.

(50) Lewis, K. E.; Golden, D. M.; Smith, G. P. *J. Am. Chem. Soc.* **1984**, *106*, 3905.

(51) (a) Ginley, D. S.; Bock, C. R.; Wrighton, M. S. *Inorg. Chim. Acta* **1977**, *85*. (b) Abrahamson, H. B.; Palazotto, M. C.; Reichel, C. L.; Wrighton, M. S. *J. Am. Chem. Soc.* **1979**, *101*, 4123.

any formation of $\text{Cp}_2\text{Cr}_2(\text{CO})_4(^{13}\text{CO})$ from $[\text{Cr}(\text{CO})_2\text{Cp}]_2$ by direct addition under these conditions. Since carbonylation of $[\text{Cr}(\text{CO})_2\text{Cp}]_2$ by 2CO is known to occur⁵¹ albeit slowly, and since $^3\text{Cp}_2\text{Cr}_2(\text{CO})_5$ (see theoretical section below) adds CO at roughly the same rate as it loses it, we conclude that the addition of CO to $[\text{Cr}(\text{CO})_2\text{Cp}]_2$ is slow to the combination of both spin state and geometric changes occurring in reaction 15.⁵²

3.1.7. Proposed Reaction Pathways for Carbonylation of $\text{N}=\text{N}=\text{CHSiMe}_3$ by $\cdot\text{Cr}(\text{CO})_3(\text{C}_5\text{R}_5)$ $\text{R} = \text{H}, \text{CH}_3$. A general mechanism in keeping with experimental studies described above and computational results described later is presented in Figure 5. The first step, 5i, is consistent with both the inhibiting effect of CO as well as the observed induction period and “S” shaped curve. This step consists of the slow loss of CO to form the radical diazo complex $\cdot\text{Cr}(\text{CO})_2(\text{N}=\text{N}=\text{CHSiMe}_3)(\text{C}_5\text{R}_5)$ in a thermodynamically unfavored associative ligand displacement reaction. In step 5ii this intermediate complex combines with a second metal radical to form an initial adduct (the structure of which is discussed in later theoretical sections) which goes on to produce $\cdot\text{Cr}(\text{CO})_2(\text{ketene})(\text{C}_5\text{R}_5)$ and $\cdot\text{Cr}(\text{CO})_2(\text{N}_2)(\text{C}_5\text{R}_5)$ by cleavage of the $\text{C}-\text{N}$ bond. One of the products of this reaction, $\cdot\text{Cr}(\text{CO})_2(\text{ketene})(\text{C}_5\text{R}_5)$ is detectable by ESR spectroscopy; however, the second product of step 5ii, $\cdot\text{Cr}(\text{CO})_2(\text{N}_2)(\text{C}_5\text{R}_5)$ is undetected and presumed to be highly reactive owing to the expected weak nature of the $\text{Cr}-\text{N}_2$ bond.⁵³ Reaction 5iii involves associative displacement of N_2 from $\cdot\text{Cr}(\text{CO})_2(\text{N}_2)(\text{C}_5\text{R}_5)$ by free $\text{N}=\text{N}=\text{CHSiMe}_3$ to reform $\cdot\text{Cr}(\text{CO})_2(\text{N}=\text{N}=\text{CHSiMe}_3)(\text{C}_5\text{R}_5)$. This is part of a reaction cycle (shown in red in Figure 5) which accounts for the “S” shaped nature of the reaction.

(52) (a) Theoretical treatment of the role of spin-state changes in organometallic reactions for mononuclear species is still evolving (see ref 52b). The authors are not aware of theoretical analysis of concomitant spin state/geometric changes being reported for metal-metal bonded systems similar to this one. (b) Carreón-Macedo, J. L.; Harvey, J. N. *J. Am. Chem. Soc.* **2004**, *126*, 5789.

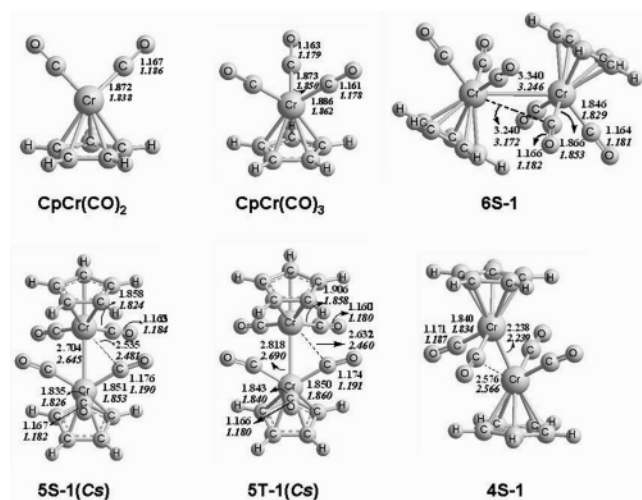


Figure 6. Computed optimized geometries of the lowest energy states for $\text{CpCr}(\text{CO})_2$, $\text{CpCr}(\text{CO})_3$, ${}^1\text{Cp}_2\text{Cr}_2(\text{CO})_6$ (**6S-1**), ${}^3\text{Cp}_2\text{Cr}_2(\text{CO})_5$ (**5T-1**), ${}^1\text{Cp}_2\text{Cr}_2(\text{CO})_5$ (**5S-1**), and ${}^1\text{Cp}_2\text{Cr}_2(\text{CO})_4$ (**4S-1**). The upper numbers (bold) were obtained by the B3LYP method, while the lower numbers (italics) were obtained by BP86.

The undetected complex “ $\cdot\text{Cr}(\text{CO})_2(\text{N}_2)(\text{C}_5\text{R}_5)$ ”⁵³ is proposed to react rapidly with a number of additional reagents depending critically on relative concentrations. Reaction 5iv results in deactivation by reaction of $\cdot\text{Cr}(\text{CO})_2(\text{N}_2)(\text{C}_5\text{R}_5)$ with CO to regenerate $\cdot\text{Cr}(\text{CO})_3(\text{C}_5\text{R}_5)$. Reaction 5v is the reaction of $\cdot\text{Cr}(\text{CO})_2(\text{N}_2)(\text{C}_5\text{R}_5)$ with $\cdot\text{Cr}(\text{CO})_2(\text{ketene})(\text{C}_5\text{R}_5)$ (the two immediate products of reaction 5ii) to form final products. Reaction 5vi, radical combination of $\cdot\text{Cr}(\text{CO})_2(\text{N}_2)(\text{C}_5\text{R}_5)$ with $\cdot\text{Cr}(\text{CO})_3(\text{C}_5\text{R}_5)$, is proposed as a major route leading ultimately to $\text{Cr}_2(\text{CO})_5(\text{C}_5\text{R}_5)_2$. Once formed, $\text{Cr}_2(\text{CO})_5(\text{C}_5\text{R}_5)_2$ can either eliminate or add CO as shown in steps 5viii and 5ix. Finally, dinuclear elimination of ketene from $\cdot\text{Cr}(\text{CO})_2(\text{ketene})(\text{C}_5\text{R}_5)$ and $\cdot\text{Cr}(\text{CO})_3(\text{C}_5\text{R}_5)$ is postulated in step 5vii.

3.2. Computational Results. 3.2.1. Structure of Mononuclear Complexes. Full analysis of ground-state and excited-state structures of the complete set of mononuclear $\text{CpCr}(\text{CO})_n$ ($n = 3, 2, 1$) and dinuclear $\text{Cp}_2\text{Cr}(\text{CO})_n$ ($n = 6, 5, 4, 3, 2, 1$) complexes by computational techniques similar to those previously reported have been performed and will be described in detail in a separate publication.⁵⁴ The focus of this section is on the structure, spin state, and energetics of those species relevant to experimental kinetic and thermodynamic data in this paper. Optimized structures computed for selected lowest energy species are shown in Figure 6; energetic data are summarized in Table 1.

(53) (a) The labile nature of the Cr–N₂ compared to the Cr–CO bond is illustrated by the fact that the complex $\text{Cr}(\text{CO})_5(\text{N}_2)$ is stable enough to be detected by fast infrared spectroscopy but decays with a first-order rate constant of 1.7 s⁻¹ (see ref 53b). This is presumably a dissociative displacement of bound N₂. In the system studied here, the Cr–N₂ absolute bond strength might be somewhat stronger, but associative displacement in the 17 e⁻ radical would make it more labile to ligand displacement by any stronger ligand. The L_M–CO bond is typically 15–20 kcal mol⁻¹ stronger than the L_M–N₂ bond for low valent complexes (see ref 53c). In addition, 18 e⁻ complexes $\text{Cr}(\text{CO})_2(\text{N}_2)(\text{arene})$ have been photochemically prepared (see ref 53d). These observations all point to expected thermochemical stability for $\cdot\text{Cr}(\text{CO})_2(\text{N}_2)\text{C}_5\text{Me}_5$ but rapid kinetic lability. Despite the reasonable nature of its postulation as a reactive intermediate in this process, there is to the author's knowledge no experimental data regarding $\cdot\text{Cr}(\text{CO})_2(\text{N}_2)\text{C}_5\text{Me}_5$. (b) Church, S. P.; Grevels, F. W.; Hermann, H.; Schaffner, K. *Inorg. Chem.* **1984**, *23*, 3830. (c) Hoff, C. D. *Prog. Inorg. Chem.* **1992**, *40*, 503. (d) Strohmaier, W.; Hellmann, H. *Chem. Ber.* **1964**, *97*, 1877.

(54) Li, Q. S.; Zhang, X.; Xie, Y.; Schaefer, H. F., III; King, R. B. Unpublished work.

Table 1. Computed Total Energies^a (kcal mol⁻¹) for Atom-Balanced Systems Relative to $\text{Cp}_2\text{Cr}_2(\text{CO})_6$ (**6S-1**) and Cr–Cr Distances by B3LYP and BP86 Methods

system	B3LYP	BP86	Cr–Cr ^b
$2\text{CpCr}(\text{CO})_2 + 2\text{CO}$	88.3	123.0	
${}^1\text{Cp}_2\text{Cr}_2(\text{CO})_4 + 2\text{CO}$	38.5	45.9	2.238, 2.239 (2.215) ^c
${}^1\text{Cp}_2\text{Cr}_2(\text{CO})_5 + \text{CO}$	29.2	36.6	2.818, 2.690
${}^3\text{Cp}_2\text{Cr}_2(\text{CO})_5 + \text{CO}$	18.8	31.7	2.704, 2.645
$2\text{CpCr}(\text{CO})_3$	1.2	17.1	
$\text{Cp}_2\text{Cr}_2(\text{CO})_6$	0	0	3.340, 3.246 (3.281) ^d

^a Energies relative to $\text{Cp}_2\text{Cr}_2(\text{CO})_6$. Data computed by conversion of calculated energies of individual species (in hartrees) by either B3LYP or BP86 method using a computed value of -113.328658 (B3LYP) or -113.327235 (BP86) hartrees for CO. Data for atom balanced systems were then subtracted from computed energy of $\text{Cp}_2\text{Cr}_2(\text{CO})_6$ (**6S-1**) which was -3156.327850 (B3LYP) or -3156.738922 (BP86) and converted from hartrees to kcal mol⁻¹. ^b Computed Cr–Cr bond distances (Å). B3LYP value is listed first, followed by BP86 value, and then experimental value (if available) in parenthesis. ^c See ref 7e. ^d See ref 7d.

The structures in Figure 6 and data in Table 1 were generated utilizing two widely accepted theoretical approaches for organometallic complexes. The computed Cr–Cr bond length for **6S-1** (~3.3 Å) and Cr≡Cr bond length **4S-1** (~2.3 Å), as shown in Table 1, are in good agreement with existing experimental data and give confidence that the calculated value for **5T-1** (~2.7 Å) is reasonable for the Cr=Cr bond length. These data are significant in that interconversion of the single, double and triple bonded complexes by either addition or elimination of CO involves not only spin changes but also significant changes in complex geometry—most notably metal–metal bond length. The relatively slow addition of CO to **5T-1** producing **6S-1** and elimination of CO from **5T-1** producing **4S-1** could possibly involve not only spin change barriers, but also concomitant geometric changes as well.

Calculated data on reaction energies taken from Table 1 provide some insight into reaction pathways, as well as the rare opportunity to compare computed and experimental data on metal–metal bond strengths. The bond dissociation energy of $\text{Cp}_2\text{Cr}_2(\text{CO})_6$ to $2\cdot\text{Cr}(\text{CO})_3\text{Cp}$ is relatively well-known: on the order of 15 kcal mol⁻¹ for both the Cp and Cp* systems.⁷ The computed values of 1.2 (B3LYP) and 17.1 (BP86) kcal mol⁻¹ differ from each other by a significant amount. The BP86 value is in reasonable accord with experiment. The computed energies of conversion of $\text{Cp}_2\text{Cr}_2(\text{CO})_6$ to $\text{Cp}_2\text{Cr}_2(\text{CO})_4 + 2\text{CO}$ of 38.5 (B3LYP) and 45.9 (BP86) kcal mol⁻¹ are considerably higher than the experimental measurement reported in this paper of ~14 kcal mol⁻¹. In this case the B3LYP is closer to the experimental result. While solvation energies can complicate the comparison of gas-phase theoretical values with solution-phase measurements, in this case solvation energies for $\text{Cp}_2\text{Cr}_2(\text{CO})_6$ and $\text{Cp}_2\text{Cr}_2(\text{CO})_4$ are likely comparable. Therefore it seems that the strength of the Cr≡Cr triple bond may be somewhat underestimated. The nature of semibridging carbonyl bonding in these complexes (in the authors' opinion) makes theoretical treatment in complexes such as $\text{Cp}_2\text{Cr}_2(\text{CO})_4$ particularly challenging.

An additional area of mechanistic interest is the energy of loss of CO from $\cdot\text{Cr}(\text{CO})_3\text{Cp}$ to form $\cdot\text{Cr}(\text{CO})_2\text{Cp} + \text{CO}$ since generation of this reactive intermediate 15e⁻ complex could conceivably play a role in diazo activation. Calculating this energy from the data in Table 1 yields a value of 43.6 (B3LYP) or 53.0 (BP86) kcal mol⁻¹. This indicates that the binding of

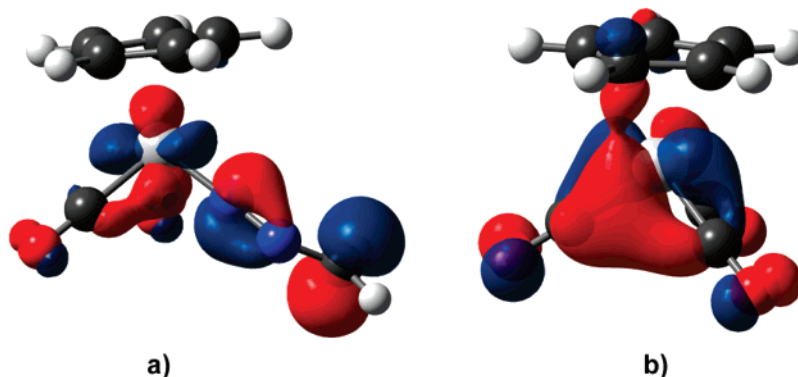


Figure 7. Drawing of the calculated SOMO for (a) $\cdot\text{Cr}(\text{CO})_2(\text{NNCH}_2)(\text{C}_5\text{H}_5)$ and (b) $\cdot\text{Cr}(\text{CO})_3(\text{C}_5\text{H}_5)$.

CO in $\cdot\text{Cr}(\text{CO})_3\text{Cp}$ may be even stronger than that in $\text{Cr}(\text{CO})_6$ for which an experimental value of 37 kcal mol^{-1} has been reported.⁵⁵

Of key importance to this paper was the calculation that the most stable state of $\text{Cp}_2\text{Cr}_2(\text{CO})_5$ is a triplet (**5T-1**) which is calculated to lie 10.4 (B3LYP) or 4.9 (BP86) kcal mol^{-1} lower than the lowest lying singlet state (**5S-1**). These data are in complete accord with experimental data which showed no NMR signal detectable for the intermediate complex formulated as $\text{Cp}_2\text{Cr}_2(\text{CO})_5$ based on its observed disproportionation to $\text{Cp}_2\text{Cr}_2(\text{CO})_4$ and $\text{Cp}_2\text{Cr}_2(\text{CO})_6$. Another key feature is the acceptable agreement between experimental and theoretical values for $\nu(\text{CO})$ frequencies utilizing the BP86 method, which in our experience appears to be more reliable for calculating $\nu(\text{CO})$ than the B3LYP method for first row transition-metal carbonyl derivatives.^{56,57} The computed infrared frequencies ($\nu(\text{CO})$ in cm^{-1} followed by intensity in parentheses) for **4S-1** of 1876 (0), 1890 (1332), 1904 (1146), and 1940 (0) are in good agreement with our measured values in toluene solution (this report) of 1878 and 1901 cm^{-1} . The intermediate from the reaction of $\text{Cp}_2\text{Cr}_2(\text{CO})_6$ and $\text{N}=\text{N}=\text{CHSiMe}_3$ suggested above to be $\text{Cp}_2\text{Cr}_2(\text{CO})_5$ exhibits a strong band at 1922 cm^{-1} , a medium band at 1832 cm^{-1} , and a weak band near 2006 cm^{-1} . These experimental values are consistent with the calculated values for the lowest energy isomer of $\text{Cp}_2\text{Cr}_2(\text{CO})_5$ (**5T-1**) of 1842 (510), 1863 (101), 1910 (917), 1925 (1828), and 1961 (9) cm^{-1} . Thus the experimentally observed medium band at 1832 cm^{-1} may correspond to the unresolved calculated $\nu(\text{CO})$ frequencies at 1842 and 1863 cm^{-1} for **5T-1**. Similarly the observed strong band at 1922 cm^{-1} may correspond to the unresolved strong calculated $\nu(\text{CO})$ frequencies at 1910 and 1925 cm^{-1} for **5T-1**. The weak band near 2006 cm^{-1} may correspond to the weak band computed to occur at 1961 cm^{-1} . Finally it should be mentioned that the calculated Cr–Cr distance in **5T-1** of 2.690 Å suggesting a $\sigma + 2/2 \pi$ Cr=Cr double bond for triplet $\text{Cp}_2\text{Cr}_2(\text{CO})_5$ is similar to the known⁵⁸ Fe=Fe double bond in the stable triplet $\text{Cp}_2\text{Fe}_2(\mu\text{-CO})_3$, which was also found to not display a measurable NMR signal.

(55) This difference could be attributed to competition by coordinated CO for electron density from the central metal atom via $\text{M} \rightarrow \text{CO} \pi^*$ back-bonding. Thus in $\text{Cr}(\text{CO})_6$ there are six CO groups competing for this electron density, whereas in $\cdot\text{Cr}(\text{CO})_3\text{Cp}$ there are only three. Backbonding would be expected to be stronger on this basis.

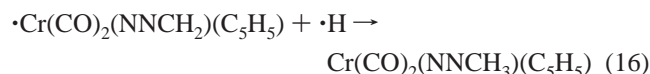
(56) Jonas, V.; Thiel, W. *J. Phys. Chem.* **1995**, *102*, 8474.

(57) Silaghi-Dumitrescu, I.; Bitterwolf, T. E.; King, R. B. *J. Am. Chem. Soc.* **2006**, *128*, 5342.

(58) Blaha, J. P.; Bursten, B. E.; Dewan, J. C.; Frankel, R. B.; Randolph, C. L.; Wilson, B. A.; Wrighton, M. S. *J. Am. Chem. Soc.* **1985**, *107*, 4561.

3.2.2. Calculation of Transition-State Structures. In place of the experimentally studied NNCHSiMe_3 the computationally simpler molecule NNCH_2 was used to calculate structures and activation energies for key intermediates using the SDD basis set with the corresponding effective core potential for chromium and the 6-311G(d,p) basis set for all the other atoms.⁵⁹ The first step in Figure 5, responsible for the induction period in the reaction and also its inhibition by CO, is substitution of a CO ligand by $\text{N}=\text{N}=\text{CHSiMe}_3$ to form $\cdot\text{Cr}(\text{CO})_2(\text{NNCHSiMe}_3)(\text{C}_5\text{H}_5)$. A molecular orbital calculation of the SOMO of a simplified model of this radical complex is shown in Figure 7. The net reaction free energy of this elementary step is 3.6 kcal mol^{-1} .

Significant spin density appears resident on the terminal C of the diazo ligand of this radical. Addition of an H atom to the proposed intermediate shown in Figure 7a would yield a methyldiazenido complex $\text{Cr}(\text{CO})_2(\text{NNCH}_3)(\text{C}_5\text{H}_5)$ as shown in



Analogous diazenido complexes of Mo and W are known.^{60,61} Formation of the diazenido complex, isoelectronic with the highly stable nitrosyl complex $\text{Cr}(\text{CO})_2(\text{NO})(\text{C}_5\text{H}_5)$ would be expected to be highly favorable. Such a radical combination would be expected to be rapid⁶² and the structure of a key reaction intermediate during step 5ii of Figure 5 is proposed to be the addition of $\cdot\text{Cr}(\text{CO})_3\text{C}_5\text{H}_5$ rather than $\cdot\text{H}$ to yield an intermediate complex $(\text{C}_5\text{H}_5)(\text{CO})_2\text{Cr}-\text{N}=\text{N}-\text{CH}_2-\text{Cr}(\text{C}_5\text{H}_5)(\text{CO})_3$. A computed structure for this proposed intermediate is shown in Figure 8. The enthalpy of addition of NO to $\cdot\text{Cr}(\text{CO})_3\text{C}_5\text{H}_5$ has been measured and indicates NO acts as a three electron donor. The Cr–NO bond strength is $33.2 \pm 1.8 \text{ kcal mol}^{-1}$ stronger than the Cr–CO bond. This driving force, plus the formation of the Cr–C bond (expected to be weak) would serve to stabilize an intermediate adduct such as that shown in

(59) (a) Calculations of transition-state structures were performed using analogous computational methods to those for stable molecules and as described in references 57b and 57c below. (b) Dolg, M.; Stoll, H.; Preuss, H.; Pitzer, R. M. *J. Phys. Chem.* **1993**, *97*, 5852. (c) Krishnan, R.; Binkley, J. S.; Seeger, R.; Pople, J. A. *J. Chem. Phys.* **1980**, *72*, 650.

(60) Herrmann, W. A. *Angew. Chem., Int. Ed. Engl.* **1975**, *14*, 355.

(61) Herrmann, W. A.; Biersack, H. *Chem. Ber.* **1977**, *110*, 896.

(62) In addition to rapid radical–radical combination reactions, studies of ultrafast disproportionation reactions of the photochemically generated radical $\cdot\text{W}(\text{CO})_3\text{C}_5\text{H}_5$ have recently been reported: Kling, M. F.; Cahoon, J. F.; Glascoe, E. A.; Shanowski, J. E.; Harris, C. B. *J. Am. Chem. Soc.* **2004**, *126*, 11414.

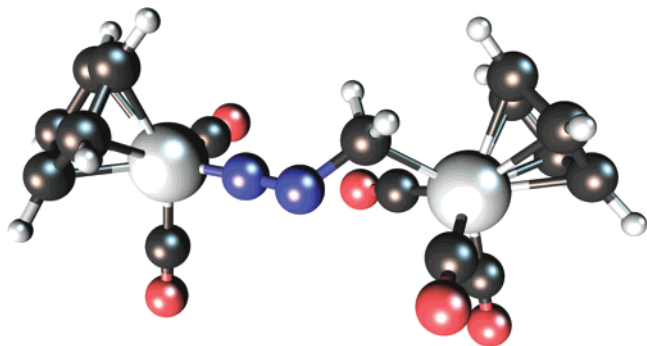


Figure 8. Calculated structure of $(\text{C}_5\text{H}_5)(\text{CO})_2\text{Cr}-\text{N}=\text{N}-\text{CH}_2-\text{Cr}(\text{C}_5\text{H}_5)(\text{CO})_3$.

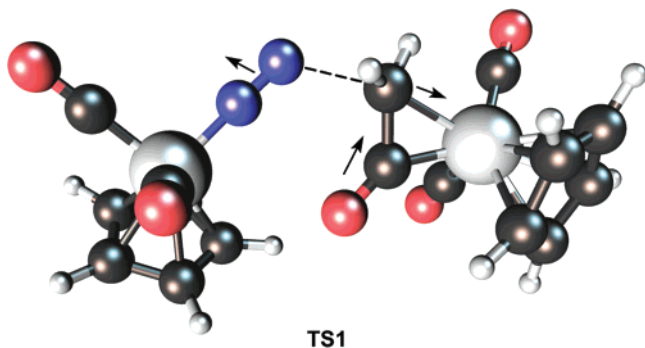


Figure 9. Computed transition state for step 5ii in the mechanism in Figure 5.

Figure 8. The related compounds $\text{M}(\text{CO})_2(\text{NNCH}_3)(\text{C}_5\text{H}_5)$ ($\text{M} = \text{Mo}, \text{W}$) are known.⁶³

The intermediate complex shown in Figure 8 is poised for formation of a C–C bond by migration of the Cr–C bond to a coordinated terminal CO. A second critical step is proposed to be migration of an alkyl radical in the bridging dinuclear intermediate, shown in Figure 8, from chromium to a carbonyl group in a manner analogous to CO insertion. As this occurs, the driving force to form ketene and N_2 provides the needed energy to split the complex to the two intermediate radicals $\cdot\text{Cr}(\text{CO})_2(\text{ketene})(\text{C}_5\text{R}_5)$ and $\cdot\text{Cr}(\text{CO})_2(\text{N}_2)(\text{C}_5\text{R}_5)$ as shown in step 5ii of Figure 5. The computed transition state is shown in Figure 9. The reaction is exothermic with a free-energy difference of $-9.3 \text{ kcal mol}^{-1}$ and proceeds with a free-energy barrier of $21.3 \text{ kcal mol}^{-1}$. Harmonic vibrational frequency calculation confirmed that **TS1** is indeed a transition state containing a single imaginary frequency ($132i \text{ cm}^{-1}$).

One possible reaction of $\cdot\text{Cr}(\text{CO})_2(\text{ketene})(\text{C}_5\text{R}_5)$ and $\cdot\text{Cr}(\text{CO})_2(\text{N}_2)(\text{C}_5\text{R}_5)$ is proposed to be recombination to reform a Cr–Cr bond and eliminate N_2 , ketene, and form $\text{Cr}_2(\text{CO})_4\text{Cp}_2$. However, as shown in Figure 9, the geometry of cleaving the C–N bond from an intermediate such as that shown in Figure 8 appears to present an initially unfavorable steric orientation to radical combination to form a Cr–Cr bond along this trajectory. Therefore it is proposed (especially for the experimentally studied complex which has a pendant SiMe_3 on the diazo carbon) that the radicals predominantly diffuse into solution rather than directly form N_2 , ketene, and $\text{Cr}_2(\text{CO})_4\text{Cp}_2$ in a single step. This is illustrated in Figure 9 and is also in accord with spectroscopic data which shows the buildup of other intermediate complexes rather than direct formation of products.

(63) Hillhouse, G. L.; Haymore, B. L.; Herman, W. A. *Inorg. Chem.* **1979**, *18*, 2423.

Two routes involving migration of the terminal CH_2 of the diazo group were also examined. The most natural way to form ketene complexes seemed to proceed via a movement of the CH_2 group toward the carbon atom of one of the CO ligands. This process, however, taking place through the transition state **TS2** (its characteristic imaginary frequency is $397i \text{ cm}^{-1}$) is predicted to be disfavored compared to the other competitive pathways owing its relatively high free energy barrier of $33.6 \text{ kcal mol}^{-1}$.

Alternatively, the electron-rich terminal methylene group of $\cdot\text{Cr}(\text{CO})_2(\text{NNCH}_2)(\text{C}_5\text{H}_5)$ may be attacked by external carbon monoxide resulting in ketene and $\cdot\text{Cr}(\text{CO})_2(\text{N}_2)(\text{C}_5\text{H}_5)$ in a highly exothermic process with a reaction free energy of $-30.4 \text{ kcal mol}^{-1}$. This concerted reaction proceeds via the transition state **TS3** (its single imaginary frequency is $346i \text{ cm}^{-1}$) with a free energy of activation of $16.8 \text{ kcal mol}^{-1}$, representing a viable pathway for ketene formation with a lower activation barrier, than for the analogous uncatalyzed reaction.²¹ The transition states involving methylene migration are depicted in Figure 10.

Despite the fact that the pathway for direct addition of CO via transition state **TS3** is computed to be low in energy, it is viewed by the authors as probably not occurring in the system studied here. For the system studied, associative displacement of the bound diazo by CO (the reverse of 5i in Figure 5) is competitive and probably has a lower activation energy than does addition of CO to the bound diazo radical as shown in **TS3**. Nevertheless **TS3** presents a viable alternative to dinuclear production. In the absence of alternative reaction channels it is expected to be competitive. Thus it is of fundamental interest and could conceivably play a role in reactions of other complexes or on surfaces.

Finally, computation of the minimum energy configuration of the intermediate complex formulated as $\cdot\text{Cr}(\text{CO})_2(\eta^2\text{ketene})(\text{C}_5\text{R}_5)$ yielded two tautomeric structures: a C,C bonded and a C,O bonded form as shown in Figure 11.

The computed energies of the C,C and C,O tautomers shown in Figure 11 are quite close, with the C,O tautomer being lower in energy by $1.3 \text{ kcal mol}^{-1}$. The $\text{CpMn}(\text{CO})_2(\text{ketene})$ complexes prepared by Herrmann and co-workers⁶ exhibit the C,C bonded form of the ketene. Work of Grotjahn has shown there is a fine balance that governs bonding in the C,C ketene, C,O ketene, and carbene + CO and other bonding motifs available in the $\text{R}_2\text{C}=\text{C}=\text{O}$ system. Infrared and ESR data do not allow for conclusive⁶⁴ assignment of which of the two binding modes shown in Figure 11 best fits experimental data. The relatively strong analogy to the manganese carbonyl complex suggests that the C,C form is the more likely structure, as well as the most likely transition state leading to the bound form of ketene as shown in Figure 9 suggests the C,C tautomer. At this point, no firm conclusion can be made regarding whether $\cdot\text{Cr}(\text{CO})_2-$

(64) Grotjahn and co-workers (see ref 4) have shown that for coordination to the $\text{IrCl}(\text{PPr}_3)_2$ fragment $\text{Ph}_2\text{C}=\text{C}=\text{O}$ coordinates in an $\eta^2\text{-C,O}$ form with $\nu\text{CO} = 1632 \text{ cm}^{-1}$, but that $\text{Ph}(\text{H})\text{C}=\text{C}=\text{O}$ coordinates in an $\eta^2\text{-C,C}$ form with $\nu\text{CO} = 1752 \text{ cm}^{-1}$. The Cr radical complex reported here has $\nu\text{CO} = 1672 \text{ cm}^{-1}$ which is somewhat closer to the C,O tautomer for Ir. However the electronic differences between the Cr and Ir complexes are large enough that no conclusion can be made at this time. Both the $\eta^2\text{-C,O}$ form and $\eta^2\text{-C,C}$ form have two approximately symmetry equivalent CO ligands. The ESR data showing hyperfine splitting from two equivalent ^{13}C nuclei derived from ^{13}CO cannot distinguish between the two forms. Use of ^{13}C labeled diazoalkane might be helpful in identifying possible coordination by this carbon (in the $\eta^2\text{-C,C}$ form), but is synthetically beyond the scope of the present study.

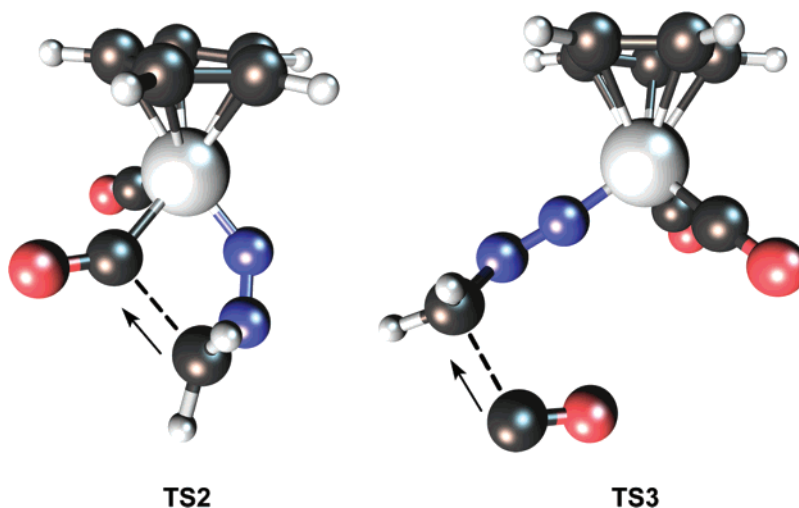


Figure 10. Computed transition states for the internal CH₂ migration (TS2) and for the intermolecular CH₂ migration step (TS3) resulting in $\cdot\text{Cr}(\text{CO})_2(\text{N}_2)(\text{C}_5\text{H}_5)$ and ketene.

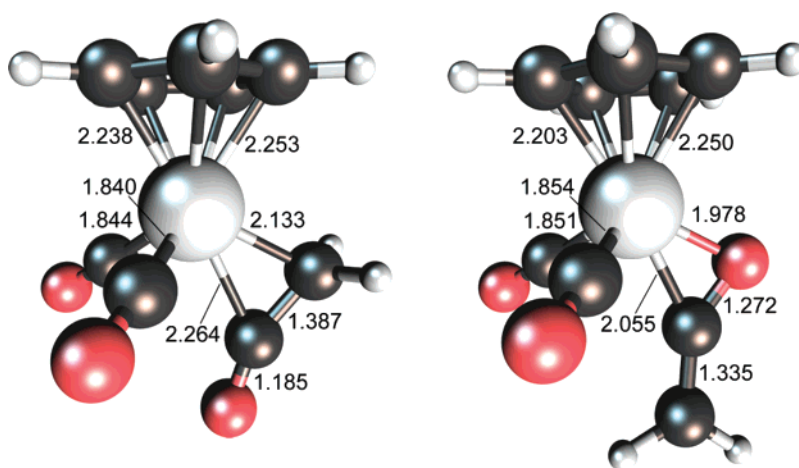


Figure 11. Calculated minimum energy structures for C,C and C,O bonded tautomers of $\cdot\text{Cr}(\text{CO})_2(\eta^2\text{-O}=\text{C}=\text{CH}_2)(\text{C}_5\text{H}_5)$. Selected bond lengths are given in angstrom.

(η^2 -ketene)(C₅H₅) is a C,C or C,O bonded tautomer. Additional experimental and computational work on this and related radical diazo alkane and ketene complexes is planned.

4. Conclusion

Combinations of theoretical and experimental approaches are used to propose a radical-based complex reaction mechanism for the seemingly simple conversion of a diazoalkane and CO to the corresponding ketene and N₂. Two key paramagnetic complexes were observed spectroscopically (triplet not actually observed directly) and supported by DFT studies, namely³ (R₅C₅)₂Cr₂(CO)₅ and $\cdot\text{Cr}(\text{CO})_2(\eta^2\text{-O}=\text{C}=\text{CHSiMe}_3)(\text{C}_5\text{R}_5)$. The rate determining step is attributed to formation of the undetected radical diazoalkane complex $\cdot\text{Cr}(\text{CO})_2(\eta^1\text{-N}=\text{N}=\text{CHSiMe}_3)(\text{C}_5\text{R}_5)$ which is then trapped by a second mole of $\cdot\text{Cr}(\text{CO})_3(\text{C}_5\text{R}_5)$ to form (C₅H₅)(CO)₂Cr–N≡N–C(H)(SiMe₃)–Cr(C₅H₅)(CO)₃ and subsequently leads to products as outlined in Figure 5. Mechanisms cannot be proven; however, the reasonable accord between theory and experiment presented here supports a concerted mechanism of this type and represents our best understanding of the complicated sequence of reactions in this system. The mechanism of carbonylation of diazoalkanes by Cr₂(CO)₆(C₅R₅)₂ reported here appears to be quite different from

that for Co₂(CO)₈ studied by Ungváry and co-workers.² Even in the well-developed field of organometallic chemistry of transition metals such as chromium and cobalt, interesting new complexes, reaction mechanisms, and theoretical understanding remain a source of surprise.

Acknowledgment. The authors dedicate this paper to Professor Ferenc Ungváry of the University of Pannonia, Hungary. Support of this work by the National Science Foundation Grants CHE-0615743 (C.D.H.) and CHE-0209857 (R.B.K.), the Hungarian Scientific Research Fund Grant No. OTKA F046959 (T.K.) and the 111 Project B07012 (Q.L.) in China is gratefully acknowledged.

Supporting Information Available: Figures S1–S10 and Table ST-1, including FTIR spectra as a function of time, ESR spectra, ¹H NMR spectra, kinetic plots and computed SOMO and spin densities for the tautomers of the proposed intermediate [$\cdot\text{Cr}(\text{CO})_2(\text{O}=\text{C}=\text{CH}_2)\text{Cp}$]; FTIR data for selected compounds and intermediates in toluene; complete ref 37. This material is available free of charge via the Internet at <http://pubs.acs.org>.

JA075008O